Journal of Economic Behavior and Organization 191 (2021) 822–845

Contents lists available at ScienceDirect

Journal of Economic Behavior and Organization

journal homepage: www.elsevier.com/locate/jebo

On the effectiveness of the European Central Bank's conventional and unconventional policies under uncertainty

Niko Hauzenberger[a], Michael Pfarrhofer[a], Anna Stelzer[b,*]

[a] University of Salzburg, Department of Economics, Mönchsberg 2A, 5020 Salzburg, Austria
[b] University of Salzburg, Salzburg Centre of European Union Studies, Mönchsberg 2, 5020 Salzburg, Austria

ARTICLE INFO

Article history:
Received 29 November 2020
Revised 7 July 2021
Accepted 25 September 2021
Available online 16 October 2021

JEL classification:
C32
E32
E52
E58

Keywords:
Euro area
Monetary policy
Bayesian smooth-transition vector autoregression
Hierarchical global-local shrinkage

ABSTRACT

In this paper, we investigate the effectiveness of conventional and unconventional monetary policy measures by the European Central Bank (ECB) conditional on the prevailing level of uncertainty. To obtain exogenous variation in central bank policy, we rely on high-frequency surprises in financial market data for the euro area (EA) around policy announcement dates. We trace the dynamic effects of shocks to the short-term policy rate, forward guidance and quantitative easing on several key macroeconomic and financial quantities alongside survey-based measures of expectations. For this purpose, we propose a Bayesian smooth-transition vector autoregression (ST-VAR), using a measure of economic policy uncertainty as signal variable. Our results suggest that transmission channels are impaired when uncertainty is elevated. While conventional monetary policy and forward guidance can be less effective during such periods, quantitative easing measures seem to work comparatively well in uncertain times.

1. Introduction

Conventional and unconventional monetary policies are widely used tools in central banks to stimulate slacking economies and counteract disinflationary pressures stemming from recessionary episodes and economic uncertainty.[1] Research measuring the effects and identifying transmission channels of monetary policy to the real and financial sectors has produced a voluminous body of literature (see, among many others, Kashyap and Stein, 2000; Kuttner, 2001; Bernanke et al., 2005; Gürkaynak et al., 2005; Sims and Zha, 2006; Tenreyro and Thwaites, 2016; Altavilla et al., 2019; Jarociński and Karadi, 2020). In this paper, we contribute to this line of work by assessing non-linear features in monetary policy transmission for the euro area (EA). We consider economic uncertainty as a key determinant of the effectiveness of policy measures enacted by the European Central Bank (ECB), and discuss factors that may render policy interventions in uncertain times less effective. A change in the monetary policy stance can be a direct reaction of the central bank to worsened economic conditions due to increases in uncertainty (e.g., lower or delayed investment and hirings when facing uncertainty shocks, see, for instance, Bloom, 2009) via changes in the policy (target) rate, or more direct and long-term market interventions

* Corresponding author.
E-mail addresses: niko.hauzenberger@sbg.ac.at (N. Hauzenberger), michael.pfarrhofer@sbg.ac.at (M. Pfarrhofer), anna.stelzer@sbg.ac.at (A. Stelzer).

[1] For a discussion of the relationship between uncertainty and conventional demand shocks that are typically counteracted by monetary policy, see Leduc and Liu (2016).

https://doi.org/10.1016/j.jebo.2021.09.041

like quantitative easing (QE). It is worth mentioning that not only domestic uncertainty, but also uncertainty-spillovers from important globalized economies may play a role in this context (see, e.g., Davidson et al., 2020).

Monetary policy can also have more subtle effects when central banks communicate their decisions and actions to the public, a phenomenon the recent literature has also referred to as so-called information effects (Nakamura and Steinsson, 2018; Bauer and Swanson, 2020; Jarociński and Karadi, 2020).[2] By transparently communicating the future path of policies and the decision makers' intentions, known as forward guidance (FG), central banks not only can reduce uncertainty about their future policy, they can also manage expectations of economic actors (Woodford, 2005). Thereby, they ensure a more effective transmission of monetary policy. Hutchinson and Smets (2017) point out how crucial the ECB's clear communication of its policy reaction function to the public was in order to improve financial and economic conditions after a period of high uncertainty in the context of the European debt crisis. Bekaert et al. (2013) also find that a looser monetary policy stance can reduce risk aversion and uncertainty.

It is however not clear *a priori* whether monetary policy works differently in times of high uncertainty when compared to low uncertainty environments. Some authors have investigated asymmetric effects of conventional monetary policy during expansions and recessions, mostly focusing on the United States (US, for examples, see Bech et al., 2014; Tenreyro and Thwaites, 2016; Dahlhaus, 2017; Angrist et al., 2018; Jannsen et al., 2019), while others examine the efficacy of QE during times of financial crises (see Kuttner, 2018; Cui and Sterk, 2019).[3] While high uncertainty levels and recessions often coincide, it is important to make a distinction between the two in the discussion of monetary policy transmission. Uncertainty can be elevated due to endogenous responses to the state of the business cycle (see Ludvigson et al., 2020). In addition, exogenous uncertainty shocks (such as the 9/11 terror attacks or, abstracting from mandatory lockdown measures, the COVID-19 pandemic) may themselves cause drops in economic activity.[4] However, it is worth reiterating that uncertainty, as well as sluggish macroeconomic and financial dynamics, can also occur without the realization of a recession.

Different circumstances surrounding an economic recession might dampen the effectiveness of monetary policy, for several reasons. First, monetary policy transmission can be impaired because financial and credit markets are dysfunctional or distressed (see Alessandri and Mumtaz, 2019). Second, persistently low short-term interest rates as a remnant of the policy reactions to previous economic recessions can lead to smaller effects of changes in interest rates on aggregate demand and output due to the presence of economic headwinds and inherent non-linearities (see Borio and Hofmann, 2017). Third, economic agents may be more hesitant to make investment or hiring decisions in times of increased uncertainty, hoping that more precise information might be available at a later point in time in order to decide on longer-term actions (Bloom, 2009). This risk aversion implies that economic agents and financial markets may be less responsive to changes in economic conditions, such as interest rates. Such conditions may be closely related to the respective level of economic uncertainty regardless of whether the economy is in expansion or recession.

This paper contributes to the existing literature on monetary policy transmission under uncertainty as follows. We empirically investigate the transmission of monetary policy conditional on the prevailing level of uncertainty in the EA. There are some studies for the case of the US (see Aastveit et al., 2017; Caggiano et al., 2017), however, to our knowledge there is no such analysis for the EA. We extend the preceding literature by including both conventional (CMP) and unconventional (UMP) monetary policy measures in our analysis (that is, we assess the effects of shocks to the policy rate, forward guidance and quantitative easing). We achieve identification by extracting exogenous variation in policies via the high-frequency instruments developed in Altavilla et al. (2019). UMP measures in particular have gained increased importance during and since the Great Recession. A key difference between our approach and the related literature on time-varying effects of monetary policy (Bech et al., 2014; Tenreyro and Thwaites, 2016; Dahlhaus, 2017; Angrist et al., 2018; Jannsen et al., 2019) is that by focusing on variation in uncertainty rather than a binary classification into economic recessions or expansions, we can observe nuanced differences in transmission channels irrespective of the fact whether an economy experienced a crisis.

From an econometric perspective, we propose a Bayesian smooth-transition vector autoregression (ST-VAR, see also Auerbach and Gorodnichenko, 2012; Granger and Terasvirta, 1993), combined with a highly flexible hierarchical shrinkage prior to obtain precise empirical inference. The econometric framework is designed to trace non-linear features of monetary policy transmission, with structural breaks in transmission channels governed by uncertainty as signal variable for determining regimes. In our empirical work, we use the economic policy uncertainty (EPU) index of Baker et al. (2016) as our measure of uncertainty. This index is constructed based on the occurrence of uncertainty-related keywords in newspapers, and designed according to a broad definition of uncertainty. To investigate different channels of monetary policy

[2] By revealing otherwise concealed information (for instance, internal staff projections by the central bank regarding the economic outlook) to consumers and financial market participants, the central bank affects and causes updates to public expectations through policy announcements.

[3] Note that empirical papers on non-linear effects of monetary policy shocks almost exclusively focus on structural breaks in transmission channels (see, e.g., Cogley and Sargent, 2005; Primiceri, 2005; Sims and Zha, 2006). Impulse response functions from VARs or local projections (see, e.g., Jordà, 2005; Ramey and Zubairy, 2018; Plagborg-Møller and Wolf, 2021) are symmetric by construction with respect to whether they are scaled to represent an expansionary or contractionary shock, and asymmetries/non-linearities arise with respect to time-varying dynamics in the conditional mean or conditional variance. A notable exception is Angrist et al. (2018), who identify asymmetric effects of positive/negative monetary policy shocks, but disregard time-varying transmission channels. In this paper, we focus on symmetric but time-varying dynamics to expansionary monetary policy shocks (determined by economic uncertainty), and leave time-varying and asymmetric dynamics for future research.

[4] Arellano et al. (2019) and Caldara et al. (2016) find contractionary effects of uncertainty shocks to be particularly large in light of tight financial conditions.

transmission, we include a set of key financial and macroeconomic variables in our model, alongside survey-based measures of expectations.

Our results suggest that conventional transmission channels are often dysfunctional in times of uncertainty. We observe time-variation governed by the uncertainty indicator in direct transmission to key interest rates, spreads and a stock market index. Similarly, both the real economy and expectations show different responses in low versus high uncertainty periods. The prevailing level of uncertainty also affects the persistence of the shocks. These findings may be explained by the fact that information effects of monetary policy play a more important role during uncertain episodes. Moreover, elevated uncertainty affects the formation of expectations of economic actors, thereby reducing the effectiveness of expectation-related transmission channels.

The remainder of the paper is organized as follows. Section 2 introduces the econometric framework used to evaluate the effectiveness of monetary policy in times of high and low uncertainty. Section 3 explains how we measure uncertainty, exogenous variation in monetary policy and provides details on the dataset. Our empirical findings are discussed and contrasted with the previous literature in Section 4. Section 5 offers closing remarks. Appendix A to Appendix D contain details on our estimation algorithm, the data and additional results. A supplementary Online Appendix presents empirical evidence on the robustness of our baseline results.

2. Econometric framework

2.1. Bayesian smooth-transition vector autoregressions

Let $\boldsymbol{y}_t$ denote an $M \times 1$-vector containing the series of interest at time $t = 1, \dots, T$. We assume a ST-VAR model of the form:

$$\begin{aligned} \boldsymbol{y}_t = &(\boldsymbol{A}_{11}\boldsymbol{y}_{t-1} + \dots + \boldsymbol{A}_{1P}\boldsymbol{y}_{t-P} + \boldsymbol{c}_1 + \boldsymbol{\delta}_{1s}x_{st}) \times S_t(u_{t-1}) \\ &+ (\boldsymbol{A}_{01}\boldsymbol{y}_{t-1} + \dots + \boldsymbol{A}_{0P}\boldsymbol{y}_{t-P} + \boldsymbol{c}_0 + \boldsymbol{\delta}_{0s}x_{st}) \times (1 - S_t(u_{t-1})) + \boldsymbol{\epsilon}_t, \end{aligned} \tag{1}$$

where $\boldsymbol{A}_{ip}$ are $M \times M$-coefficient matrices for state $i \in \{0, 1\}$ and lag $p = 1, \dots, P$, and $\boldsymbol{c}_i$ is an $M \times 1$-vector of intercepts. The state indicators $S_t(u_{t-1}) \in [0, 1]$ transition smoothly between regimes and depend on a signal variable u_{t-1} (in our case, a measure of uncertainty). They are bounded between zero and one and discussed in more detail below. $\boldsymbol{\epsilon}_t \sim \mathcal{N}(\boldsymbol{0}, \boldsymbol{\Omega})$ is a Gaussian error term with zero mean and $M \times M$-covariance matrix $\boldsymbol{\Omega}$.[5]

We include CMP and UMP shocks (indexed $s \in \{\text{TG}, \text{FG}, \text{QE}\}$, with target/policy rate, TG; forward guidance, FG; and quantiative easing, QE) one at a time as scalar exogenous instrument x_{st} (for details how these instruments are constructed, see Section 3.2). The $M \times 1$-vector $\boldsymbol{\delta}_{is}$ measures the contemporaneous responses of the endogenous variables to the shock s, and is thus the state-specific impact vector that can be used for structural inference (for details, see Paul, 2020).

The ST-VAR has several attractive properties when contrasted with related econometric approaches. Compared to deterministic regime classifications, threshold or Markov switching (MS) models, with potentially only a small number of observations in one of the regimes, the ST-VAR informs its parameter estimates based on a continuum of regimes with the support of each regime being bounded between zero and one (loosely related to probabilities). This sharpens inference, and pushes the model towards a linear specification. When compared to conventional time-varying parameter (TVP) models with gradually evolving coefficients (that is, with a random walk state equation), using our specification with a pre-defined (exogenous) signal variable u_{t-1} allows to link time-variation to observed factors.[6]

A crucial modeling decision for the ST-VAR is both the choice of the signal variable u_{t-1} and the transition function for $S_t(u_{t-1})$. In our empirical work, we use the economic policy uncertainty index of Baker et al. (2016) as u_{t-1}, and discuss this indicator in more detail in Sections 3 and 4. For selecting the transition function, we follow the related literature (see, e.g., Auerbach and Gorodnichenko, 2012; Caggiano et al., 2014) and choose:

$$S_t(u_{t-1}) = \frac{1}{1 + \exp\left(-\phi(u_{t-1} - \gamma)\right)},$$

a first-order logistic function, with u_{t-1} denoting the first lag of our measure of uncertainty. We include the signal variable as first lag to avoid any contemporaneous feedback from policy actions depending on whether we are in a low/high uncertainty regime. Moreover, we standardize u_{t-1} to have zero mean and unit variance prior to estimation, to render the parameter ϕ scale-invariant (see also Gefang and Strachan, 2009).

[5] Earlier research on the EA has shown that evidence for time-variation in the volatility of key series is muted (see, for instance, Jarociński and Lenza, 2018). Such features are mainly required for data from the United States, when jointly modeling distinct periods such as the Great Inflation (approximately 1965–1982) versus the Great Moderation (around 1985–2007), see, e.g., Clark (2011). Accordingly, we follow the recent literature on EA monetary policy analysis using a homoscedastic specification, see for instance, Burriel and Galesi (2018) or Jarociński and Karadi (2020). For these reasons, we refrain from introducing regime-switching covariance matrices. Moreover, it is worth noting that our identification approach is independent of the covariance matrix (different to Auerbach and Gorodnichenko, 2012 or Caggiano et al., 2014), which implies that even though we rule out time-varying volatilities, the impacts of the shocks feature time-variation.

[6] Recent papers overcome this shortcoming of conventional TVP models by augmenting the state equations of the TVPs by latent or observed factors (Chan et al., 2020; Fischer et al., 2021). This allows for addressing why specific parameters change over time, similar to our interpretation of the signal variable driving changes in the parameters, and thus, impulse responses.

The parameter $\phi > 0$ governs the speed of adjustment, while γ marks a threshold value that separates the two regimes. Naturally, depending on the actual evolution of the signal variable u_{t-1}, the parameter γ determines the split at which observations are allocated more to either state zero or one. The parameter ϕ governs how smoothly the economy transitions between states. In the limiting case with $\phi \to \infty$, the state indicator $S_t(u_{t-1})$ switches between zero and one (marking clearly separated regimes), closely related to conventional threshold VARs (see, e.g., Alessandri and Mumtaz, 2019; Huber and Zörner, 2019). For the case of $\phi \to 0$, the logistic function turns constant, with $S_t(u_{t-1}) = 0.5$ effectively resulting in a linear VAR specification.

2.2. Prior setup

2.2.1. Priors for the state-specific VAR coefficients

Our proposed prior setup for the autoregressive coefficients is similar to Hauzenberger et al. (2021) who use a MS vector error correction model. While MS models produce a strictly binary regime allocation – $S_t(u_{t-1})$ would either be zero or one at time t – our setup implies that the coefficient matrices are weighted averages across the two states. We design our prior to be centered on the corresponding linear specification of our model and pool coefficients across regimes.

To achieve this, we collect the regime specific coefficients in $\boldsymbol{A}_i = (\boldsymbol{A}_{i1}, \dots, \boldsymbol{A}_{iP}, \boldsymbol{c}_i, \boldsymbol{\delta}_i)$ for states $i \in \{0, 1\}$, and construct $\boldsymbol{a}_i = \text{vec}(\boldsymbol{A}_i)$ of size $J = (M(MP+2)) \times 1$. The prior variances are collected in $\tilde{\boldsymbol{V}}_i = \text{diag}(\{\tilde{v}_{ij}\}_{j=1}^{J})$ and $\boldsymbol{V} = \text{diag}(\{v_j\}_{j=1}^{J})$ with $\tilde{v}_{ij} = \tilde{\lambda}_i^2 \tilde{\psi}_{ij}^2$ and $v_j = \lambda^2 \psi_j^2$. We propose a hierarchical global-local shrinkage setup based on the horseshoe (HS, Carvalho et al., 2010) prior:[7]

$$\boldsymbol{a}_i \sim \mathcal{N}(\tilde{\boldsymbol{a}}, \tilde{\boldsymbol{V}}_i), \quad \tilde{\lambda}_i \sim \mathcal{C}^+(0,1), \quad \tilde{\psi}_{ij} \sim \mathcal{C}^+(0,1), \tag{2}$$

$$\tilde{\boldsymbol{a}} \sim \mathcal{N}(\boldsymbol{a}, \boldsymbol{V}), \quad \lambda \sim \mathcal{C}^+(0,1), \quad \psi_j \sim \mathcal{C}^+(0,1), \tag{3}$$

for $i \in \{0, 1\}$ and $j = 1, \dots, J$. The symbol $\mathcal{C}^+$ denotes the half-Cauchy distribution. Equation (2) states that the regime-specific coefficients arise from a Gaussian distribution with mean $\tilde{\boldsymbol{a}}$, and shrinkage is governed by two regime-specific shrinkage parameters collected in $\tilde{\boldsymbol{V}}_i$.

The first is a global shrinkage parameter, $\tilde{\lambda}_i$, which pushes all coefficients in $\boldsymbol{a}_i$ towards $\tilde{\boldsymbol{a}}$, and thus, a linear model specification. The second type are local scaling parameters, $\tilde{\psi}_{ij}$, that allow for variable-specific deviations from linearity in each regime. Rather than choosing specific values for $\tilde{\boldsymbol{a}}$, we assign a Gaussian prior centered on $\boldsymbol{a}$ and estimate these coefficients, see Eq. (3). We choose a prior mean of 0.95 for all first-order autoregressive coefficients in $\boldsymbol{a}$ if the respective series is transformed as log-levels, and set it to zero in all other cases, mimicking a Minnesota-type prior (Doan et al., 1984; Litterman, 1986). Choosing 0.95 rather than unity implies that our prior is centered on a stationary multivariate model. We introduce another hierarchy of shrinkage on the common mean via $\boldsymbol{V}$ to regularize the high-dimensional parameter space. Again, we rely on the HS prior and consider a global shrinkage parameter λ alongside local scalings ψ_j.

Intuitively, our setup implies that we impose conventional shrinkage towards a stylized prior model on the linear specification's parameters in $\tilde{\boldsymbol{a}}$. In a second step, we impose regime-specific shrinkage of the non-linear coefficients towards the linear model. Our setup differs from Hauzenberger et al. (2021) based on our choice of the respective shrinkage prior. Introducing additional global shrinkage parameters by regime implies that our model is capable of detecting a regime-specific degree of shrinkage, which is particularly useful if observations are unevenly distributed across states.

2.2.2. Priors for the variance-covariance matrix

Our model has a potentially huge-dimensional parameter space, which quickly becomes computationally prohibitive to sample in one block when the number of endogenous variables (M) or the lag order (P) increases. To alleviate the computational burden, we rely on triangularizing the model to allow for equation-by-equation estimation (see Carriero et al., 2019). Appendix A shows how to write the multivariate system of equations as a set of M independent regressions.

To establish our prior, we decompose the covariance matrix of the error $\boldsymbol{\epsilon}_t$ in Eq. (1) as $\boldsymbol{\Omega} = \boldsymbol{H}\boldsymbol{\Sigma}\boldsymbol{H}'$ with $\boldsymbol{H}$ denoting the normalized lower Cholesky factor of $\boldsymbol{\Omega}$ and $\boldsymbol{\Sigma} = \text{diag}(\{\sigma_m^2\}_{m=1}^{M})$ is an $M \times M$ matrix with equation-specific variances σ_m^2, for $m = 1, \dots, M$, on its diagonal.

We collect the free elements (those below the diagonal) of the matrix $\boldsymbol{H}$ in an $R = (M(M-1)/2) \times 1$-vector $\boldsymbol{h}$ and index its elements by h_r with $r = 1, \dots, R$. Here, we define an $R \times R$-matrix $\hat{\boldsymbol{V}} = \text{diag}(\{\hat{v}_r\}_{r=1}^{R})$ with $\hat{v}_r = \hat{\lambda}^2 \hat{\psi}_r^2$ and impose a HS prior:

$$\boldsymbol{h} \sim \mathcal{N}(\boldsymbol{0}, \hat{\boldsymbol{V}}), \quad \hat{\lambda} \sim \mathcal{C}^+(0,1), \quad \hat{\psi}_r \sim \mathcal{C}^+(0,1). \tag{4}$$

Again, the global parameter $\hat{\lambda}$ imposes shrinkage towards zero for all free elements of the matrix $\boldsymbol{H}$, while the local parameters $\hat{\psi}_r$ allow for deviations of the rth coefficient.

On the diagonal elements of $\boldsymbol{\Sigma}$, we impose a set of M weakly informative independent inverse Gamma priors:

$$\sigma_m^2 \sim \mathcal{G}^{-1}(3, 0.3), \quad \text{for } m = 1, \dots, M.$$

[7] We choose the horseshoe prior due to its excellent shrinkage properties and the lack of a prior tuning hyperparameter. Note that any prior from the class of global-local shrinkage priors (see, e.g., Cadonna et al., 2020) can be used.

2.2.3. Priors for the state transition function

In our empirical application, we standardize the signal variable u_{t-1} such that it has mean zero and unit variance. We construct the prior for the threshold parameter γ such that it is bounded between the minimum and maximum values of u_{t-1} and center it on zero:[8]

$$\gamma \sim \mathcal{TN}\big(0, \sigma_\gamma^2, \min(u_{t-1}), \max(u_{t-1})\big).$$

We choose $\sigma_\gamma^2 = 0.01$ implying an informative prior. This prior information is needed to impose a sensible regime-allocation in our model. It is worth mentioning that while the prior pushes the parameter towards zero, likelihood information may still overrule the tightness of the prior, different to using hard-coded restrictions as in Auerbach and Gorodnichenko (2012).

The speed of adjustment parameter follows a Gamma distribution:

$$\phi \sim \mathcal{G}(a^2/b, a/b).$$

The hyperparameters are chosen such that a denotes the mean of the prior and b its variance. We set $a = 2$ with variance $b = 0.01$. This implies that the economy spends about 25% of the time in the high-uncertainty regime. A similar reasoning for introducing substantial prior information as for γ applies here. Calibrating the prior in this manner imposes a sensible regime-allocation in our model, yet we still obtain a posterior distribution for the parameter and deviations from the prior are possible if likelihood information prevails in the respective posterior.

This completes our prior setup. Combining the priors with the likelihood of the model results in a set of mostly standard conditional posterior distributions that can be used for Gibbs sampling. For the parameters of the state transition function, we rely on a Metropolis-within-Gibbs step. These can be used for designing a Markov chain Monte Carlo (MCMC) algorithm to obtain posterior inference. Details on the resulting posterior distributions and the sampling algorithm are provided in Appendix B.

3. Data and model specification

3.1. Uncertainty, real, financial and survey-based variables

As our measure for EA wide uncertainty u_{t-1}, we use the economic policy uncertainty (EPU) index developed by Baker et al. (2016) on the log-scale.[9] This newspaper-based index is chosen because it captures a broad definition of uncertainty (as opposed to strictly focusing on either macroeconomic or financial uncertainty). A comparison of uncertainty indices for the EA and its countries is provided in Rossi and Sekhposyan (2017) or Azqueta-Gavaldón et al. (2020). Since the index shows upward trending behavior in its raw format, we detrend and standardize it prior to including it in our model (that is, the resulting measure has zero mean and unit variance). We achieve this by regressing the series on a linear trend term, and consider the residuals of this regression as our signal variable. When used without these adjustments, the index essentially splits our sample into pre- and post-sovereign debt crisis regimes.

Our detrending procedure allows to capture deviations of uncertainty from a hypothetical long-run equilibrium, thereby accounting for the fact that economic agents may react endogenously to prolonged periods with high levels of uncertainty and specific uncertainty-related events. For related studies on endogenous movements of uncertainty, see Carriero et al. (2018) and Ludvigson et al. (2020). By contrast, the detrended series marks increases/decreases of uncertainty relative to a baseline level, providing a more adequate picture of uncertainty episodes.

The vector of endogenous variables, $\boldsymbol{y}_t$, contains several macroeconomic and financial time series, alongside survey-based measures of expectations. In particular, we include the Euribor three-month rate (E3M) as our short-term target rate. To trace the effects of FG and QE shocks, we also consider two-year (GBY2, targeted by the FG factor) and ten-year (GBY10, targeted by the QE factor) EA government bond yields. Our set of financial indicators is completed by the Euro Stoxx 50 stock market index (ES50), and the ICE BofA Euro high-yield index option-adjusted spread (OAS) to measure financial conditions.

As key macroeconomic indicators, we include the harmonized index of consumer prices (HICP), the unemployment rate (UNEMP) and industrial production excluding construction (IP) as a monthly indicator of economic activity. To gauge the impact of monetary policy shocks on firms and household expectations, we refer to the following survey-based measures. We include industrial (ISICI) and consumer confidence (CSCCI) indicators, consumers' unemployment expectations over the next twelve months (CSU12), and consumer opinions on the future tendency of inflation (CIE). The baseline set of variables also includes our aforementioned measure of uncertainty as endogenous variable. Details on data sources and a priori transformations are provided in Appendix C. The number of endogenous variables is $M = 13$. We choose a lag length of $P = 4$.

3.2. Measuring monetary policy shocks and identification

We state in Eq. (1) that monetary policy shocks are included in our model as exogenous instruments x_{st}. In this paper, we assess both CMP and UMP shocks following the methodology set forth in Altavilla et al. (2019), relying on the *Euro Area*

[8] Centering the standardized signal variable on zero implies a prior centered on the mean of u_{t-1} in the scale of the non-transformed series.

[9] The series is available for download from policyuncertainty.com.

Monetary Policy Event-Study Database (EA-MPD).[10] Before discussing how the instruments are established, we provide a brief overview on ECB communication that can be exploited for high-frequency identification.[11]

ECB policy decisions are typically communicated to the public in a two-step process. First, there is a press release which provides information on the policy decision (without discussing how the Governing Council came to this decision). Second, the press release is followed by a press conference 45 min later, where the President reads a prepared statement explaining the previously announced policies (which takes about 15 min), and answers questions in a Q&A session afterwards (about 45 min). The latter is often informative about the ECB's outlook and the future path of monetary policy. In conjunction, these two "monetary events" and precise time-stamps are employed to identify different policy surprises on financial markets and thus provide a measure of exogenous variation in monetary policy.

The EA-MPD collects high-frequency market reactions in narrow windows (ten minutes before and after the event) around both monetary events, based on tick data for interest rates at different maturities and stock returns, among others. In essence, if monetary policy actions by the ECB were fully anticipated by market participants, we should observe no reaction of asset prices during either the press release or the press conference. If, however, the ECB communicates unanticipated actions (that are thus orthogonal to the information set of the public), the market would quickly adjust and price this new information. Altavilla et al. (2019) exploit these dynamics in a wide range of asset classes using an identified factor model (subject to orthogonality restrictions), and pin down four different shocks: the *target, timing, forward guidance* and *quantitative easing* shock.[12]

In this paper, we rely on these factors to trace the transmission of both CMP and UMP shocks to the real and financial economy in times of uncertainty. We select the target (TG), forward guidance (FG) and quantitative easing (QE) as our shocks of interest and include them in our model as exogenous instruments:[13]

- *Target* (TG): The TG shock is derived from announcements during the press release. This factor does not load on surprises during the press conference window, implying that the series captures mainly CMP. In terms of relevant instruments, the factor exhibits loadings on short-term yields, with a maximum loading on the one-month overnight index swap (OIS) rate.
- *Forward guidance* (FG): The FG factor loads on series during the press conference window, and mostly affects the middle segment of the yield curve (with a peak effect at about two years of maturity and substantial loadings up to five years). The FG factor captures revisions in market expectations about the future path of monetary policy that are orthogonal to the TG factor's current policy surprise content. We interpret this shock series as the first measure of UMP.
- *Quantitative easing* (QE): The QE shock is designed to dominate in the press conference window. This factor shows maximum loadings for yields with ten-year maturity, reflecting the long end of the yield curve. It is worth mentioning that based on the identifying restrictions of the factor model, QE is only present after 2014, consistent with the historical evolution of asset purchase programmes by the ECB. We interpret this shock as our second measure of UMP.

The exogenous shocks x_{st} for $s \in \{\text{TG}, \text{FG}, \text{QE}\}$ are included one at a time in our model set forth in Eq. (1), and the vectors $\boldsymbol{\delta}_{i,\text{TG}}$, $\boldsymbol{\delta}_{i,\text{FG}}$ and $\boldsymbol{\delta}_{i,\text{QE}}$ measure the sensitivity of the endogenous variables in $\boldsymbol{y}_t$ to these shocks in regime $i \in \{0, 1\}$. Using the identified contemporaneous responses, we can calculate higher-order impulse response functions by tracing the impacts through the dynamic multivariate system. This approach to identifying the dynamic impact of monetary policy shocks is similar to Gertler and Karadi (2015) and Paul (2020).

An important aspect of monetary policy analysis using high-frequency data are the aforementioned central bank information effects (see, for instance, Nakamura and Steinsson, 2018; Jarociński and Karadi, 2020).[14] In a nutshell, it is argued that central bank announcements not only convey the respective policy decision, but also reveal information about the projected economic outlook. Jarociński and Karadi (2020) investigate information effects in detail for the EA by assessing the high-frequency responses of three-month OIS rates in conjunction with Euro Stoxx 50 movements around announcement dates. They find that positive comovement in both surprises is indicative of an information shock, and impulse responses look substantially different when compared to those of a pure monetary policy shock (with negative comovement of the surprise series, in line with theory).[15]

Miranda-Agrippino and Ricco (2021) propose a procedure for pre-processing instruments, by purging them from predictable components, to achieve clean identification of monetary policy shocks which yields similar results. By contrast, Bauer and Swanson (2020) find that what Nakamura and Steinsson (2018) call information shocks (capturing differences in public and private information on the economic outlook of the central bank) might actually be artefacts of economic agents

[10] Raw event-study data is available at ecb.europa.eu/pub/pdf/annex/Dataset_EA-MPD.xlsx. The dataset is described in detail in Altavilla et al. (2019).

[11] An early paper on high-frequency identification of monetary policy shocks using tick-frequency asset price data is Kuttner (2001). Related methods have subsequently been used for monetary policy analysis, with some examples covering both the US and the EA given by Bernanke and Kuttner (2005), Gürkaynak et al. (2005), Brand et al. (2010), Jarociński and Karadi (2020), Andrade and Ferroni (2021) and Hauzenberger and Pfarrhofer (2021).

[12] For details on identification, see also Gürkaynak et al. (2005), Brand et al. (2010) and Swanson (2021).

[13] The timing shock is very similar to the forward guidance shock, with the only difference being the time horizon for which forward guidance is applicable. To economize on space, we focus on the forward guidance instrument aimed at the two-year ahead horizon discussed below.

[14] Note that the derivation of the factors we use as instruments is unaffected by the presence of information shocks (Altavilla et al., 2019).

[15] In this context, Campbell et al. (2012) and Andrade and Ferroni (2021) decompose observed monetary policy surprises into a *Delphic* and a *Odyssean* component with both being orthogonal to each other. While the former represents a *pure* information shock, the latter isolates the actual monetary policy component.

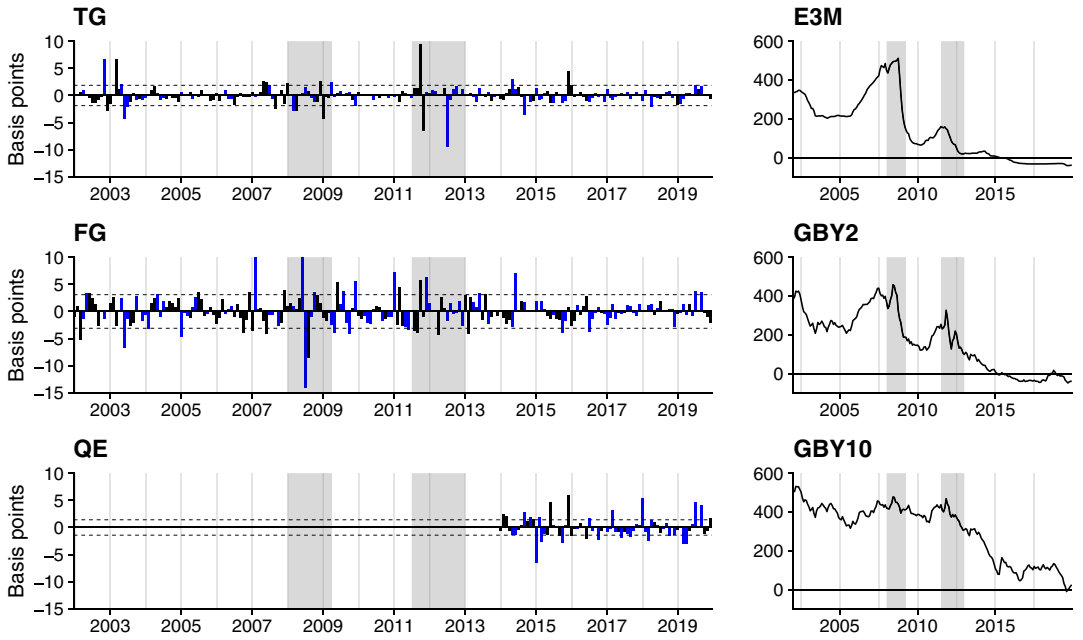

Fig. 1. Exogenous instruments (target/policy rate, TG; forward guidance, FG; quantitative easing, QE), signaling effects and interest rates at different maturities. The bars indicate the respective value of the factor per month. Bars in blue show months where at least one policy announcement resulted in positive comovements of high-frequency surprises in three-month OIS rates and the Euro Stoxx 50 stock index (information shock). Black bars show negative comovements of these two high-frequency series (conventional monetary policy shock in line with theory), see also Jarociński and Karadi (2020). The dashed lines mark one standard deviation of the shocks. The grey shaded areas indicate recessions dated by the CEPR Euro Area Business Cycle Dating Committee. (For interpretation of the references to colour in this figure legend, the reader is referred to the web version of this article.)

and the central bank reacting to the same news shock. Given the close relationship between uncertainty and news shocks (Berger et al., 2020), this might be one of the channels why the effectiveness of monetary policy is affected during periods of elevated uncertainty.

While our econometric framework in principle allows for disentangling monetary policy from information shocks and tracing the impacts of both individually,[16] we refrain from doing so, for three reasons:

1. We closely follow Altavilla et al. (2019), who use the external instruments directly for identifying TG, FG and QE shocks in their financial VAR analysis. Our two-regime model is equipped for endogenously selecting distinct regimes, similar to their sub-sample analysis where they detect the presence of potential information shocks.
2. The informational content and role of information shocks in the context of FG and QE is less clear than when focusing solely on TG shocks (see the discussion in Bauer and Swanson, 2020). Putting specific restrictions on reactions may in fact bias estimates of the actual shocks.
3. Our paper intends to shed light on the transmission of CMP and UMP in times of uncertainty. It seems a worthwhile empirical exercise to study the transmission of the actual measures of our exogenous shocks to the real and financial economy over time. And this transmission also includes the presence of information effects during policy announcements by the ECB. The information effects potentially impaired the effectiveness of policies during specific times, for instance, when uncertainty levels were elevated. We elaborate on this notion in the context of the discussion of our results below.

In fact, Bauer and Swanson (2020) argue that " even though high-frequency monetary policy surprises may be correlated with macroeconomic data *ex post*, they still can be used, without adjustment, to estimate the effects of an exogenous change in monetary policy [...]." To ensure that our factors are valid external instruments for our shocks of interest, we follow Miranda-Agrippino and Ricco (2021) and project out *ex post* correlation with the information set contained in the ST-VAR. We achieve this by regressing the instruments on its own P lags and the contemporaneous values of the variables in $\boldsymbol{y}_t$ and P of their lags, and use the residuals from this regression as the respective instrument.

Figure 1 plots the exogenous instruments (TG, FG and QE) and corresponding interest rates (three-month Euribor, E3M; EA two-year government bond yields, GBY2; EA ten-year government bond yields, GBY10; see also next sub-section) on a monthly frequency. The figure is adjusted to indicate months where information effects may have played a role during

[16] One could, for instance, employ the approach referred to as *poor man's sign restrictions* by Jarociński and Karadi (2020). This implies that for months where high-frequency surprises move in the same direction, the factors would be set to zero. A major drawback of this strategy is that months are binarily classified as either *pure* monetary policy or information shocks, ruling out cases in between.

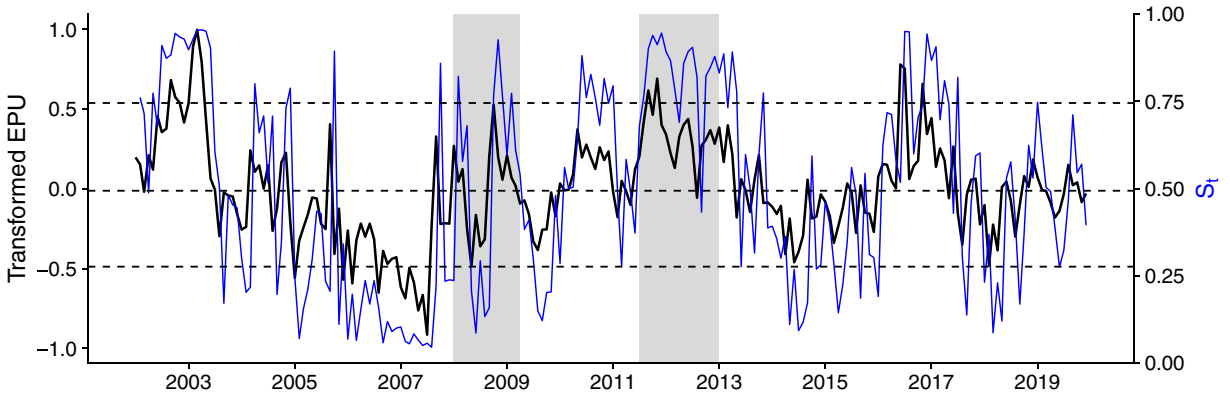

Fig. 2. Transformed uncertainty measure u_{t-1} and the posterior median of state allocation S_t. The left axis shows our detrended and demeaned measure of uncertainty (economic policy uncertainty, EPU) on the log-scale (left axis, in solid black). The right axis refers to the state allocation $S_t \in [0, 1]$ over time (right axis, in solid blue). Note that the posterior median of $S_t(u_{t-1})$ closely mirrors the series implied by the expected values of our priors on γ and ϕ, which is due to informativeness of our prior setup (see Section 2.2). The dashed horizontal lines mark the 5th, 50th and 95th percentile of the uncertainty index over time, which we subsequently label the low, medium and high uncertainty scenario in the context of our impulse response analysis. The grey shaded areas indicate recessions dated by the CEPR Euro Area Business Cycle Dating Committee. (For interpretation of the references to colour in this figure legend, the reader is referred to the web version of this article.)

ECB policy announcements. The months with potential information shocks are marked in blue (based on at least one policy announcement during the respective month resulting in positive comovements of the three-month OIS rate and Euro Stoxx 50 surprises).

Several findings are worth noting. First, the largest movements in both the TG and FG factor are visible during the two crisis episodes (the Great Recession and the subsequent European debt crisis). Second, while we observe positive comovement shocks throughout our sample, they occur most frequently during crisis episodes and after 2015. These crisis episodes are also often accompanied by elevated levels of uncertainty. While we discuss this aspect in more detail below in the context of our structural results, we conjecture that this may be one of the reasons why monetary policy during uncertain times appears to be less effective. Positive comovement shocks tend to cancel the effects of conventional monetary policy (see Jarociński and Karadi, 2020). Third, the QE factor is only active after 2014. Here, we observe information shocks particularly around 2015 and at the end of the sample. Fourth, one striking observation when considering the corresponding interest rates is that rate cuts do not necessarily result in surprises in the instrument of the same sign. Positive surprises, for example, occur if financial markets expected larger cuts than realized. While the ECB intended to conduct expansionary policy, the less-than-expected cuts act like contractionary shocks.

4. Empirical results

4.1. Uncertainty indicator and state allocation

Figure 2 shows the evolution of the transformed measure of uncertainty (solid black, left axis). The right axis refers to the state allocation $S_t(u_{t-1}) \in [0, 1]$ over time (in solid blue). For this plot, we show the posterior median state allocation of $S_t(u_{t-1})$. Note that the posterior distribution closely mirrors the series implied by the expected values of our priors on γ and ϕ, which is due to the previously discussed informativeness of our setup.

We start with discussing the uncertainty index. Highest values are observed early in the sample, in the build-up to Gulf War II starting in 2003. From 2005 until the onset of the Great Recession, a period of relatively low uncertainty emerges. Just before and during the Great Recession we observe several peaks in economic policy uncertainty, related to several fiscal and monetary policy measures intended to calm financial markets and foster economic recovery. Between the two major recessions of our sample, the index first lowers around 2009, but suddenly increases again in early 2010. The elevated levels in 2010 mark substantial increases in sovereign credit risk throughout Europe. These dynamics culminate during the most severe years of the European debt crisis between 2012 and 2013. While we observe a brief period of lower uncertainty after 2014, the index again increases around the Brexit referendum in mid-2016 in the United Kingdom. After 2017, the index fluctuates around its unconditional mean. Note that in line with our previous reasoning, elevated uncertainty and economic recessions often coincide, but higher uncertainty levels are not confined to recessionary episodes.

Turning to $S_t(u_{t-1})$, we find that the main features of the uncertainty index translate closely to our bounded indicator. It is worth mentioning that several periods appear to be more persistent when compared to the measure of uncertainty. While peaks and troughs in the EPU index often yield values of $S_t(u_{t-1})$ close to one and zero respectively, a substantial period is characterized by values in between. Using the bounded indicator rather than interacting the endogenous variables of the VAR directly with uncertainty allows for estimating clearly separated low/high uncertainty regimes. While this may

also be achieved via MS models, our approach has the advantage that we also take into account "normal" times where we neither observe particularly high nor low levels of uncertainty. We thereby combine the two advantages of both interacted and MS-VAR models in our framework. This implies that conditional on the respective level of uncertainty, we can estimate time-varying effects of CMP and UMP.

4.2. Conventional and unconventional monetary policy under uncertainty

Our econometric framework allows to calculate impulse response functions at each point in time. This implies that both impact reactions and transmission dynamics governed by the transitioning VAR coefficients may differ over time, conditional on the uncertainty indicator. It is worth mentioning that Altavilla et al. (2019) find that EA financial market participants do not perceive monetary policy effects to be asymmetric regarding positive/negative surprises in terms of asset prices responses. This implies that our regime-allocation and responses will not be driven by monetary policy shocks being predominantly positive/negative in times of varying levels of uncertainty.

To obtain relative impulse responses to the shocks indexed $s \in \{\text{TG}, \text{FG}, \text{QE}\}$, we let ς_s denote the standard error of x_{st}. Moreover, let $\boldsymbol{M}_i$ denote the $MP \times MP$ companion matrix for regime $i \in \{0, 1\}$ based on the VAR in Eq. (1),[17] and define the companion-form impact vector $\tilde{\boldsymbol{\delta}}_{is} = (\varsigma_s \boldsymbol{\delta}_{is}', \mathbf{0}_{1\times[(M-1)P]})'$. By multiplying $\boldsymbol{\delta}_{is}$ with ς_s we obtain responses reflecting a one standard deviation shock to the instrument.

The framework allows for two different variants of impulse responses for shock s at horizon h (for $h \geq 0$). Denote by u_τ the τth unconditional percentile of the uncertainty indicator u_{t-1} over time. Let $\tau \in \{0.05, 0.5, 0.95\}$, with 0.05, 0.5 and 0.95 referring to low, medium and high uncertainty levels. The impulse response function can be computed as

$$\mathbf{IRF}_{s0,\tau} = \boldsymbol{J}\tilde{\boldsymbol{\delta}}_{\tau s} = \boldsymbol{J}\Big(S_t(u_\tau)\tilde{\boldsymbol{\delta}}_{1s} + (1 - S_t(u_\tau))\tilde{\boldsymbol{\delta}}_{0s}\Big),$$

$$\mathbf{IRF}_{sh,\tau} = \boldsymbol{J}(\boldsymbol{M}_1 \times S_t(u_\tau) + \boldsymbol{M}_0 \times (1 - S_t(u_\tau)))^h \tilde{\boldsymbol{\delta}}_{\tau s}, \quad \text{for } h > 0.$$

These results are shown in the following sub-sections in the form of boxplots.

Our framework also allows to compute impulse response functions at time t, conditional on the actual level of uncertainty u_{t-1}:

$$\mathbf{IRF}_{s0,t} = \boldsymbol{J}\tilde{\boldsymbol{\delta}}_{ts} = \boldsymbol{J}\Big(S_t(u_{t-1})\tilde{\boldsymbol{\delta}}_{1s} + (1 - S_t(u_{t-1}))\tilde{\boldsymbol{\delta}}_{0s}\Big),$$

$$\mathbf{IRF}_{sh,t} = \boldsymbol{J}(\boldsymbol{M}_1 \times S_t(u_{t-1}) + \boldsymbol{M}_0 \times (1 - S_t(u_{t-1})))^h \tilde{\boldsymbol{\delta}}_{ts}, \quad \text{for } h > 0.$$

where $\boldsymbol{J}$ is an $M \times MP$-dimensional matrix that selects the first M rows of a vector of dimension $MP \times 1$. These and additional empirical results (impulse response functions over time and alternative horizons, as well as several robustness checks involving alternative measures of uncertainty and an alternative prior setup), can be found in the supplementary Online Appendix. Note that all results are qualitatively robust. Alternative uncertainty measures sometimes yield significant results when our benchmark index does not, providing evidence for the validity of our results as a lower bound of the effects of monetary policy under uncertainty. These differences may arise from variations in the definition of the respective index, e.g., whether it targets policy or financial uncertainty. In all figures, we distinguish shocks by the respective colors of the impulse response functions. TG shocks are in shades of blue, FG shocks in red and QE shocks in green.

4.2.1. The target/policy rate shock

The first set of results shows the responses to a CMP shock in Fig. 3, captured by the target factor in the form of boxplots. This figure (as do those for the FG and QE shock) collect the responses of variables in a low (L), medium (M) or high (H) uncertainty state, as well as the difference (D) in responses between the low and high uncertainty state. The L, M, H scenarios are based on the $\tau \in \{0.05, 0.5, 0.95\}$ unconditional percentile of the uncertainty indicator over the full sample. The rectangle refers to the 25th and 75th percentile of the posterior distribution (interquartile range), the posterior median is indicated as solid line and the whiskers mark the 68% posterior credible set. The left-hand side panels (a) show responses on impact, the right-hand side panels (b) show responses at the one-year ahead horizon. For numerical values of the impulse response functions in a table, see Appendix D.

To assess direct effects of monetary policy shocks on financial quantities, consider the first column of panel (a) in Fig. 3. Recall that the responses are scaled to reflect a one standard deviation shock to the instrument. An expansionary CMP shock results in a contemporaneous decrease of the main policy rate E3M, irrespective of the level of uncertainty. In times of lower uncertainty, a one standard deviation TG shock results in a decrease of 1.4 basis points (BPs) of the targeted interest rate. Contrary, when uncertainty is higher, E3M decreases by 0.8 BPs. The difference between the high and low uncertainty state is small, but positive. For the responses of E3M at the one-year horizon, refer to the first column of panel (b) in Fig. 3. We observe an increase of the short term interest rate for all uncertainty-scenarios. However, they are not significantly different from zero, and the difference between high and low uncertainty levels is insignificant as well.

[17] That is, the first M rows of this matrix are the VAR coefficients in $\boldsymbol{A}_i$ and the remaining rows yield an identity.

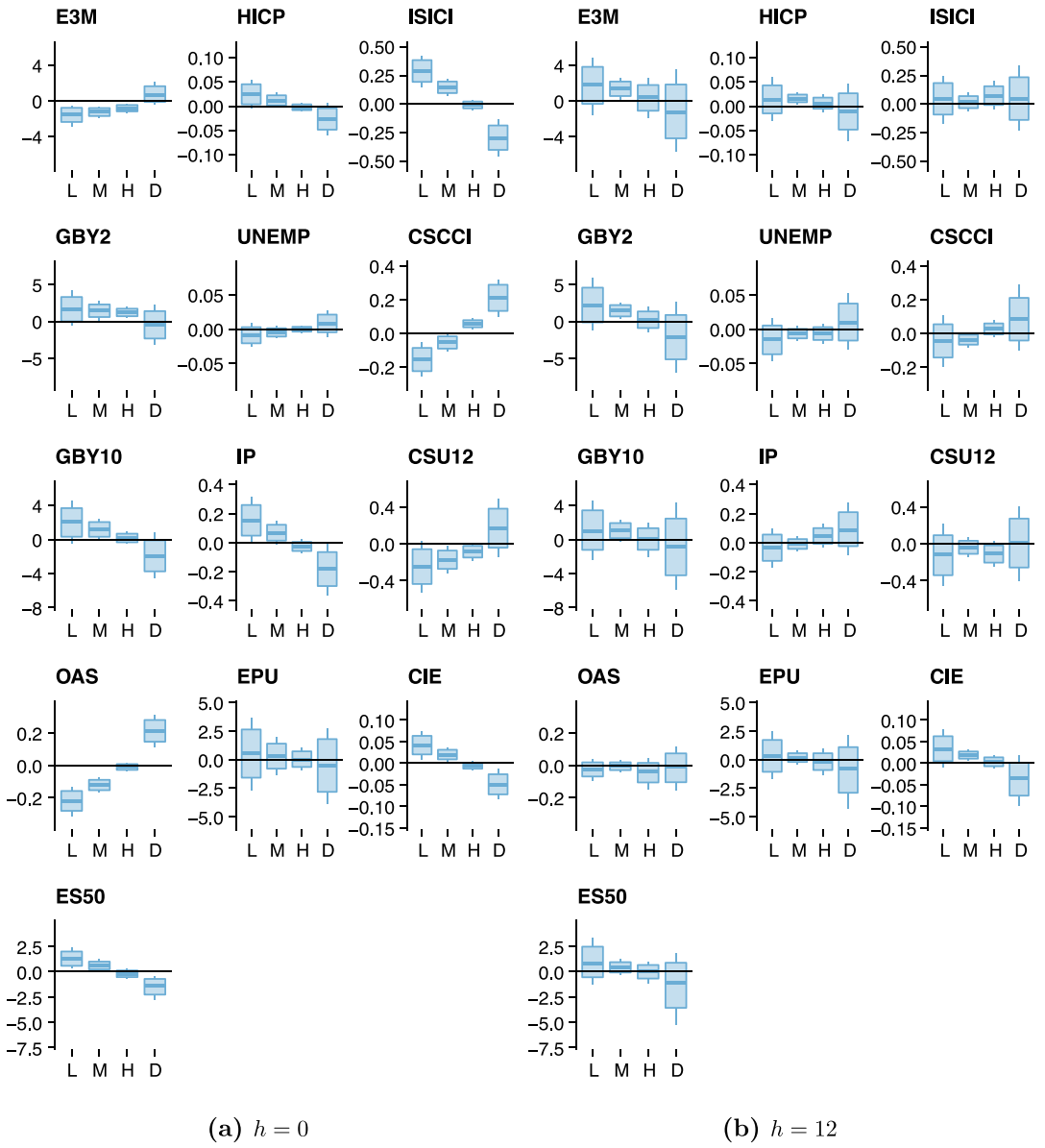

Fig. 3. Boxplots of the impulse response functions to the target/policy rate shock for different levels of uncertainty on impact and one-year ahead. Impulse response functions are summarized in form of a boxplot. The rectangle marks the 25th and 75th percentile of the posterior distribution (interquartile range), the posterior median is indicated as solid line; the whiskers of the plot refer to the 68% posterior credible set. Panel (a) shows responses on impact, panel (b) at the 12 month horizon. We display responses in the low (L), medium (M) or high (H) uncertainty state, as well as the difference (D) in responses between L and H. The L, M, H scenarios are based on the $\{0.05, 0.5, 0.95\}$ unconditional quantile of the uncertainty indicator over time. A description of the variables and transformations is provided in Appendix C.

Two-year yields (GBY2) show increases on impact for all considered levels of uncertainty. While two-year yields react more strongly when uncertainty is lower, with a median response of a 1.7 BPs versus 1.3 BPs increase respectively, the difference in responses in times of higher uncertainty is again not statistically significantly different from zero. A comparable dynamic can be observed for ten-year government bond yields (GBY10). In particular, we find that positive impact reactions for longer-maturity yields are again stronger during periods of low uncertainty. However, contrary to the medium-maturity yields, the results show that the difference in responses between low and high levels of uncertainty has substantial posterior mass on values below zero. For both two-year and ten-year yields, the effects of an expansionary TG shock seem to be rather short lived, since at the one-year horizon, responses of these rates revert back to zero. However, as a general trend, at the one-year horizon, some posterior mass is shifted to positive values in times of low and medium levels of uncertainty, indicating that responses in more uncertain times are less persistent.

Turning to OAS, our measure capturing the tightness of financial conditions, we observe several interesting findings. While the impulse response for this variable is significantly negative for periods of low uncertainty, it is muted and even insignificant during times of higher uncertainty. While expansionary shocks decrease spreads (which is in line with theory), this channel appears to be impaired under uncertain economic conditions. Our final financial variable is the Euro Stoxx 50 index (ES50), where the scale is in percent. Again, we detect variation in the impact response. In periods where uncertainty is lower, we observe slightly positive effects and a 1.2% increase, in line with the related literature. During high-uncertainty periods, where spreads also show muted reactions, we detect even a slightly negative effect of expansionary policy on stock prices, resulting in a significant negative difference in responses between high and low uncertainty. While this may seem puzzling, we conjecture that this finding relates to information effects occurring particularly under uncertainty. As suggested by Jarociński and Karadi (2020), information shocks may reverse the responses of CMP shocks, thereby muting or even producing wrong-sided responses. We argue that this is one of the reasons why conventional monetary policy appears to be less effective when uncertainty is elevated. Similar to the preceding discussion of interest rates, the responses of both OAS and ES50 revert to zero around the one-year horizon.

Following our discussion of direct effects measured with financial variables, we proceed with investigating the effects on several key macroeconomic quantities in the second column of the left- and right-hand side panel of Fig. 3. The impaired transmission of CMP shocks on financial quantities during times of higher uncertainty carries over to these real economic indicators. While all our responses are in line with economic theory, the magnitude of the responses differs substantially conditional on the prevailing level of uncertainty.

We find that inflation and economic activity (measured by industrial production) increase on impact after an expansionary shock during low-uncertainty episodes as expected. However, when uncertainty is high, we often measure insignificant effects. For both inflation and economic activity, this yields significant negative differences in responses between the high and low uncertainty scenario. The same is true for the unemployment rate, albeit with reversed sign, reflecting that expansionary shocks translate to decreases in unemployment. We detect this in the case of responses for low uncertainty levels. When uncertainty is elevated, CMP appears to be less effective, and we find that unemployment does not react significantly to changes in the policy rate. The uncertainty measure, on the other hand, does not react contemporaneously to CMP in a significant manner regardless of the prevailing level of uncertainty. For all macroeconomic variables we again observe that an expansionary target shock does not result in persistent responses, as all variables show insignificant responses at the one-year horizon.

These findings are roughly in line with Aastveit et al. (2017), who evaluate US monetary policy shocks in times of high and low uncertainty. Within their framework, they also find that effects of monetary policy tend to be much smaller when uncertainty is high. Indeed, they find that monetary policy effects on real economic activity are approximately halved when their measure of uncertainty is in its upper decile as compared to it being in this bottom decile, and the difference is statistically significant. Similarly, Caggiano et al. (2017) find that the stabilizing effects of monetary policy after an uncertainty shock seem to be greater in times of expansion, rather than contraction. This indicates that our results on the effects of CMP for the case of the EA, conditional on different levels of uncertainty, are in line with the existing literature on the US.

Our final set of results for survey-based expectations in response to the TG shock are displayed in the third column of panels (a) and (b) in Fig. 3. We detect substantial variation in impact responses conditional on the uncertainty indicator. Responses for most variables are again muted and mostly insignificant under higher uncertainty. This points towards impaired transmission channels of monetary policy during these episodes. Industrial, unemployment and inflation expectations show insignificant responses during uncertain times, while impacts are substantial when uncertainty is low. Industrial confidence and inflation expectations increase after an expansionary TG shock, while unemployment expectations decrease. This finding may be linked to Coibion et al., 2018, who find that expectation formation is often based on imperfect information. We conjecture that it is harder to update expectations in light of high levels of uncertainty, resulting in insignificant results for the high-uncertainty scenario. The difference in impact responses between low and high uncertainty levels is significantly different from zero for all these survey-based expectations.

A puzzling result appears for consumer expectations. Here, we find that during uncertain episodes, confidence increases in response to expansionary shocks as expected. During more certain times, however, consumer confidence appears to decrease after such a shock on impact. It is worth noting that results for the three-month and six-month time horizon (provided in Appendix D) show that consumer confidence seems to react with some delay, increasing at the 3-month horizon and reaching its peak at the six-month horizon. While most responses of expectations peter out around the one-year ahead horizon, inflation expectations show more persistent effects in times of low or medium uncertainty. This relates to the survey-based findings for a randomized-controlled trial by Coibion et al. (2019), who identify substantial cross-sectional dispersion of inflation expectations. This suggests that while some consumers can correctly identify monetary policy actions, others cannot, and this translates to persistent effects of the shocks.

Summarizing, we find that an expansionary CMP shock results in comparable decreases in interest rates for different levels of uncertainty, but translates to looser financial conditions more efficiently in times of low uncertainty. Stock returns even show negative effects in times of elevated uncertainty. These results carry over to indicators of the real economy. Episodes of low uncertainty show textbook reactions of real variables like inflation, economic activity and unemployment to an expansionary CMP shock. By contrast, in times of higher uncertainty, we often find insignificant effects. As for our variables of survey-based expectations, again, CMP seems to affect expectations less in times of high uncertainty. All these findings point to the conclusion that CMP is a relevant and efficient tool in times of low or medium uncertainty. However,

its transmission to financial markets, real economic activity and expectations is impaired when uncertainty is higher. Transmission via investment or consumption channels, such as the direct interest rate channel, the intertemporal substitution effect or wealth effects (Mishkin, 1996; Boivin et al., 2010), are likely sources of these differentials. Our results suggest that one reason for this is that consumers do not change their inflation expectations after a CMP shock hits the economy when uncertainty is high. As the real interest rate rather than the nominal interest rate determines asset prices and spending, it is possible that changed dynamics in the formation of inflation expectations in times of high uncertainty also lead to different or even diverging dynamics between real and nominal interest rates, resulting in hindered transmission of CMP. Overall, all these findings are in line with existing literature that suggest that real option effects from theory may exist and that elevated uncertainty leads economic agents to form expectations not rationally or perfectly informed, and perhaps, even to postpone decision making until uncertainty decreases.

4.2.2. The forward guidance shock

Turning to our first set of results capturing the effects of UMP, we discuss our results for the FG shock based on the results displayed in Fig. 4. Again, we imposean expansionary one standard deviation shock to the instrument. Note that in this case, the policy relevant variable is the two-year government bond yield (GBY2), since the underlying factor is designed to load strongly on this maturity. Indeed, we find the strongest reaction to the shock for the two-year government bond yield, which decreases by about one BP on impact in times of low uncertainty and by about 1.6 BPs when uncertainty high. Similar to the CMP shock discussed above, we detect only muted variation conditional on the prevailing level of uncertainty in the short-term rate and the two-year yield. While all three interest rates react negatively on impact (a key difference when compared to the TG shock), the ten-year government bond yields do so more strongly in times of elevated uncertainty. Interestingly, and also different to the CMP shock, the spreads do not show significant reactions at any horizon we consider. While overall dynamics appear to be similar for stock prices, we detect negative responses of equities under uncertainty and positive responses in certain times, resulting in a significant difference between the two. This finding again points to the notion of information effects playing a role in impairing the transmission of monetary policy during times of uncertainty.

In line with the forward looking character of this UMP instrument, we detect more persistent effects of the FG shock, particularly for interest rates. Especially responses for medium levels of uncertainty exhibit significant negative effects even at the three-year ahead horizon (available in the paper's Online Appendix). Interestingly, variation for higher-order impulse responses in the case of the short-term rate and two-year yields is muted, different to the CMP shock.

The second column of both panels in Fig. 4 displays the responses of the macroeconomic variables to the FG shock on impact and at the one-year horizon. In this context, we obtain several puzzling results. While we again find significant effects of the policy shock for inflation mainly during comparatively certain times, they exhibit the wrong sign on impact. For times of higher uncertainty, we find considerable posterior mass on a positive response, resulting in a significant difference between certain and uncertain times. Assessing the three to six-month horizon (see Appendix D), we observe that the sign of the HICP response reverses for both certain and uncertain times. The difference in responses between a certain and a more uncertain state remains significantly different from zero up until the one-year horizon. The responses for industrial production have the correct sign, but are insignificant to a muted degree of variation across uncertainty scenarios. Different to CMP, we observe significant impact effects of FG on our uncertainty measure. While expansive forward guidance lowers uncertainty in low uncertainty periods, it appears to increase uncertainty during episodes of elevated uncertainty. In terms of persistence of the shocks, we observe only a brief half-life of FG on macroeconomic quantities (with the exception of the aforementioned more persistent effects on HICP), with most shocks being either insignificant on impact, or petering out quickly between the one-quarter and one-year ahead horizon.

In our final set of results for the survey-based measures, we again detect several puzzling effects in the third column of panels (a) and (b) in Fig. 4. We measure negative effects in industry and inflation expectations as response to an expansive shock, albeit they are small in size and barely significant. It is worth mentioning that impact responses for industry, unemployment and inflation expectations are the same irrespective of the level of uncertainty. Consumer confidence differs substantially, with negative responses during elevated periods of uncertainty, and positive estimates when uncertainty is low. This finding is in line with the argument that FG conveys information about the future stance of the economy to households and consumers. The puzzling effects tend to fade away for higher-order responses, with industry, consumer inflation and unemployment expectations exhibiting the expected sign at the three-month ahead horizon in times of lower uncertainty. For all variables measuring expectations, we can observe a certain degree of variation with respect to the level of uncertainty up until the one-year horizon when all responses turn insignificant. It is worth pointing out that consumer inflation expectations react negatively to an expansive FG shock in more uncertain times until the six month horizon. Again, we note that consumer expectations are subject to substantial cross-sectional dispersion (Coibion et al., 2019), and this response may be an artefact of a substantial number of households being unable to update their expectations accurately.

4.2.3. The quantitative easing shock

Our final set of results is concerned with an expansionary QE shock. The impulse response functions are again scaled to reflect a one standard deviation increase of the instrument. Since the respective QE factor is only active after 2014, we restrict our sample to the period where this policy measure is relevant. The results are shown in Fig. 5.

Starting again with financial quantities, we observe that by construction of the instrument, impact reactions of the short-term rate are muted and increase with longer maturities. We detect the largest effects for ten-year yields during periods of

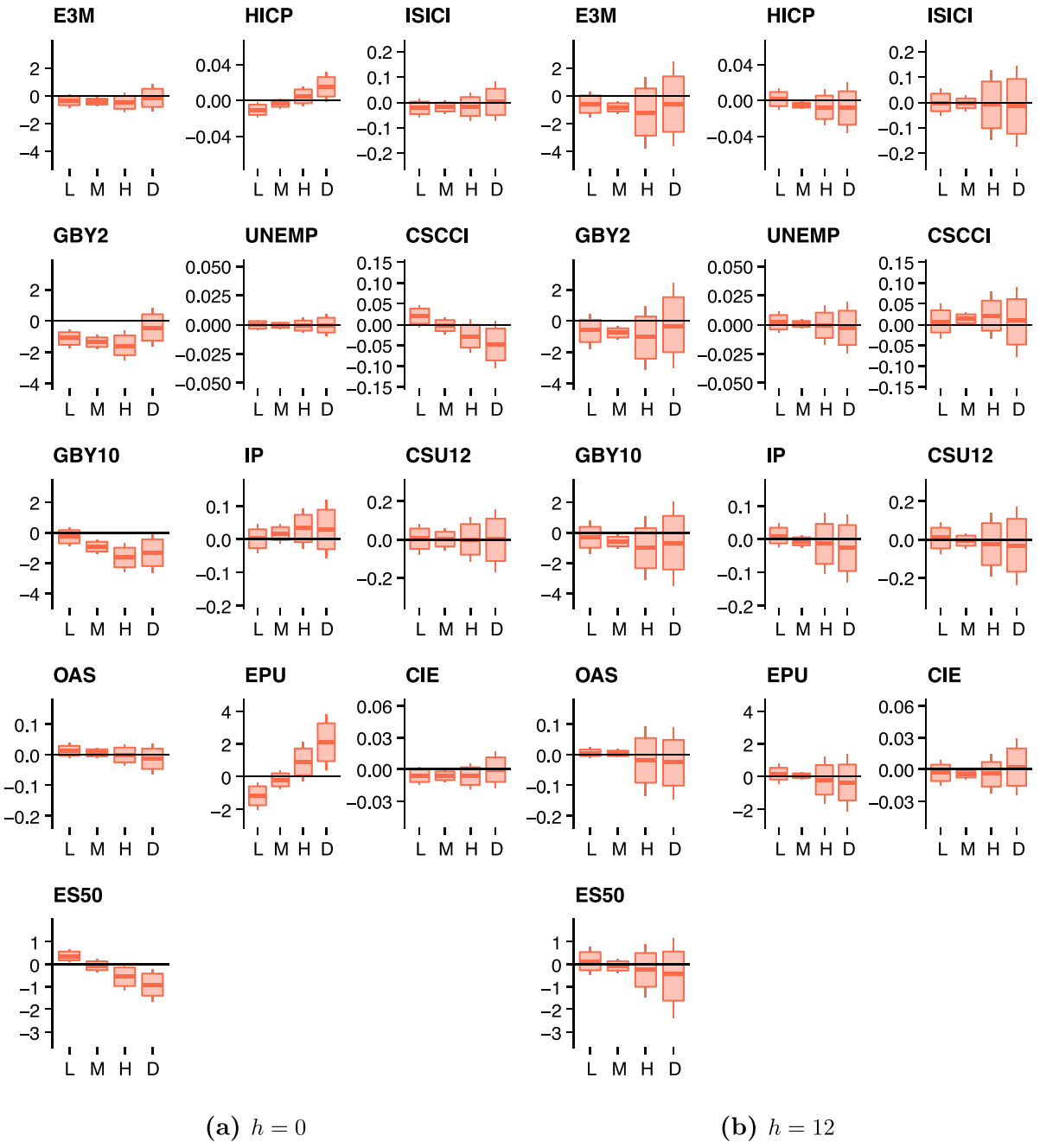

Fig. 4. Boxplots of the impulse response functions to the forward guidance shock for different levels of uncertainty on impact and one-year ahead. Impulse response functions are summarized in form of a boxplot. The rectangle marks the 25th and 75th percentile of the posterior distribution (interquartile range), the posterior median is indicated as solid line; the whiskers of the plot refer to the 68% posterior credible set. Panel (a) shows responses on impact, panel (b) at the 12 month horizon. We display responses in the low (L), medium (M) or high (H) uncertainty state, as well as the difference (D) in responses between L and H. The L, M, H scenarios are based on the $\{0.05, 0.5, 0.95\}$ unconditional quantile of the uncertainty indicator over time. A description of the variables and transformations is provided in Appendix C.

low uncertainty, with GBY10 decreasing by about three BPs. Similar to the FG shock and in contrast to TG, we observe insignificant reactions of OAS, our variable measuring financial conditions. In line with the literature (see, e.g., Swanson, 2021), effects on the stock market are also muted. In terms of higher-order responses, we observe that all variables that do not show significant impact reactions do not turn significant at any horizon or any uncertainty level. It is worth mentioning that the shocks are more short-lived when compared to FG, with two-year yield decreases turning insignificant after one quarter, and ten-year yields returning to the baseline after about six months.

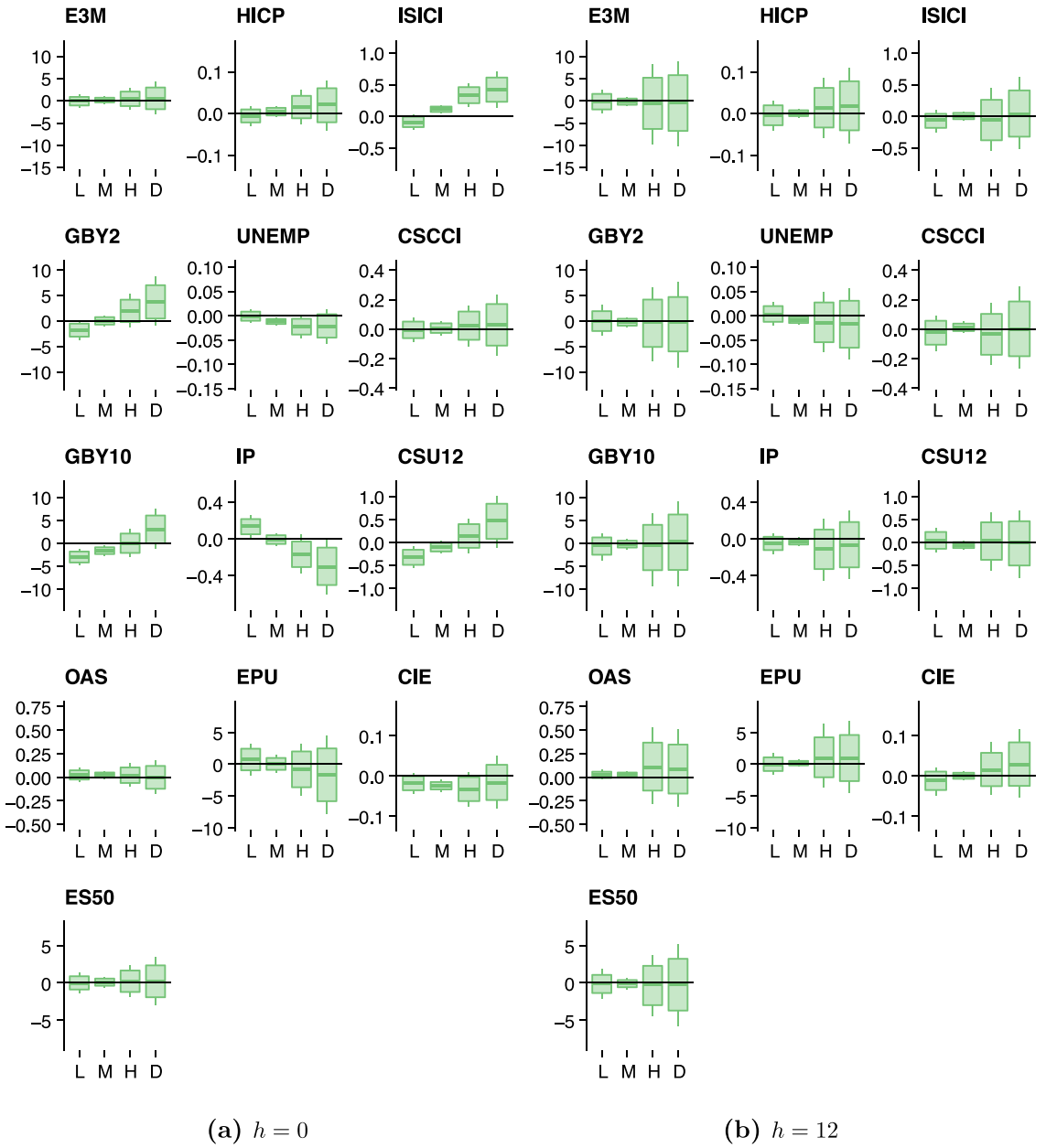

Fig. 5. Boxplots of the impulse response functions to the quantitative easing shock for different levels of uncertainty on impact and one-year ahead. Impulse response functions are summarized in form of a boxplot. The rectangle marks the 25th and 75th percentile of the posterior distribution (interquartile range), the posterior median is indicated as solid line; the whiskers of the plot refer to the 68% posterior credible set. Panel (a) shows responses on impact, panel (b) at the 12 month horizon. We display responses in the low (L), medium (M) or high (H) uncertainty state, as well as the difference (D) in responses between L and H. The L, M, H scenarios are based on the $\{0.05, 0.5, 0.95\}$ unconditional quantile of the uncertainty indicator over time. A description of the variables and transformations is provided in Appendix C.

The results for our set of macroeconomic variables are displayed in the second column of both panels in Fig. 5. We detect minor differences in the responses conditional on the level of uncertainty for all series we consider. Interestingly, we find that estimated effects are somewhat larger if uncertainty is high. During times of elevated uncertainty, an expansionary shock translates to a modest increase of inflation (albeit insignificant) and substantial decreases of unemployment. When uncertainty is at a low or medium level, however, we observe insignificant responses for these variables. Economic activity measured by industrial production tends to increase if uncertainty is low. The uncertainty index does not exhibit significant responses across impulse horizons and over time. One minor puzzling result of negative industrial production responses when uncertainty is high reverses for one-quarter ahead impulses. Unemployment effects are comparatively persistent in

times of higher uncertainty, with effects with considerable posterior mass on negative values for up to the six-month ahead horizon.

Our discussion of the empirical results is completed by investigating the responses of the survey-based expectation measures in Fig. 5. Similar to the macroeconomic variables, we find that for variables where we detect significant effects, they are larger in magnitude during periods of elevated uncertainty. An expansionary QE shock results in increases particularly for industry confidence when uncertainty is elevated, but decreases industry confidence when there is less uncertainty in the economy. Impact reactions for consumer confidence are insignificant, but turn significant for the one-quarter ahead horizon. Again, when uncertainty is low, the expansionary QE shock lowers consumer confidence, but when there is high uncertainty, it actually increases the confidence measure, resulting in a significant difference between the two uncertainty states. The timing of the response is also interesting for unemployment expectations. While impact reactions are stronger during low-uncertainty periods and insignificant for high uncertainty, this changes at the one-quarter ahead horizon with substantially larger effects in times of uncertainty. The difference in responses between high and low uncertainty, however, is only significantly different from zero on impact. Similar as in the context of the FG shock, we detect a puzzle for consumer inflation expectations, with negative effects on impact, independent of the level of uncertainty, that peter out after six to twelve months. It is worth mentioning that the QE shock results in impulse responses with only little persistence, with all effects turning insignificant at the latest after one year.

Summarizing our results on UMP, we find that both FG and QE shocks exhibit expected effects on interest rates of different maturity. While the effects of the FG shock seem to be less affected by the prevailing level of uncertainty, effects of QE are more efficiently transmitted to interest rates in episodes of higher uncertainty. Similarly, QE effects on the real economy and expectations seem to be larger when uncertainty is elevated. Here, both the portfolio rebalancing channel as well as the policy signalling channel may play a role in the transmission of QE (see Hutchinson and Smets, 2017). Our results imply that this instrument appears to be particularly suited for periods characterized by high levels of uncertainty, which is in line with conclusions drawn in the previous literature (see, for example Kuttner, 2018; Cui and Sterk, 2019).

5. Closing remarks

In this paper, we assess the effectiveness of several conventional and unconventional monetary policy measures by the ECB conditional on the prevailing level of uncertainty. We measure effects of target, forward guidance and quantitative easing shocks over time with a smooth-transition vector autoregressive model using uncertainty as a signal variable. This allows for obtaining non-linear impulse response functions of a set of financial, macroeconomic and survey-based expectation variables to the shocks.

Our results suggest that transmission channels are impaired in times of uncertainty, especially for conventional monetary policy. We conjecture that this is due to two major reasons. First, high levels of uncertainty change the impact effects of the shocks by changing direct transmission to key financial variables such as spreads. We argue that this phenomenon may be related to the presence of central bank information effects during these periods that accompany monetary policy announcements. Second, we find that the prevailing level of uncertainty at the time of the shock affects the persistence of the effects. The persistence of the shocks is dependent on the specific instrument, but is also variable specific. Our results suggest that especially the effectiveness of transmission channels related to industrial and consumer expectations are affected in times of uncertainty.

The effectiveness of policy measures also depends crucially on the respective tool invoked by the central bank. Conventional policy measures appear to be affected particularly negatively by high uncertainty. By contrast, unconventional measures such as large-scale asset purchases appear to work comparatively better in times of high uncertainty. For both UMP measures, our analysis suggests that there might be beneficial complementarities between TG, FG and QE. On the one hand, FG might be useful in combination with a CMP instrument, making its effects more persistent and more robust with respect to different uncertainty levels. On the other hand, a QE shock in combination with CMP might not only add to the effects of a change in the target rate via the portfolio rebalancing and signaling channel, but it might also make up for deficiencies in the transmission of CMP in times of elevated uncertainty.

Declaration of Competing Interest

None. The authors declare no conflict of interest.

Acknowledgements

We thank Florian Huber for valuable comments and suggestions, and Guiseppe Ragusa for providing us with an update of the conventional and unconventional monetary policy factors extracted from the monetary policy event-study database (EA-MPD). All authors gratefully acknowledge financial support from the Austrian Science Fund (FWF, grant no. ZK 35). Hauzenberger acknowledges funding by the Oesterreichische Nationalbank (project no. 18127), Pfarrhofer also acknowledges funding by the Oesterreichische Nationalbank (project no. 18304), and Stelzer acknowledges financial support by funds of the Humer Foundation.

Appendix A. Equation-by-equation estimation

In this Appendix we outline the estimation of our smooth transition VAR model in Eq. (1). For notational simplicity, we first collect the respective coefficient matrices in an $M \times K$-matrix, where $K = 2(MP + 2)$, and the regressors (i.e., lagged dependent variables and the exogenous instrument) in a $K \times 1$-vector:

$$\boldsymbol{A} = (\boldsymbol{A}_{11}, \dots, \boldsymbol{A}_{1P}, \boldsymbol{c}_1, \boldsymbol{\delta}_1, \boldsymbol{A}_{01}, \dots, \boldsymbol{A}_{0P}, \boldsymbol{c}_0, \boldsymbol{\delta}_0),$$
$$\boldsymbol{z}_t = \Big((\boldsymbol{y}'_{t-1}, \dots \boldsymbol{y}'_{t-P}, 1, x_{st}) \times S_t(u_{t-1}), (\boldsymbol{y}'_{t-1}, \dots \boldsymbol{y}'_{t-P}, 1, x_{st}) \times (1 - S_t(u_{t-1}))\Big)'.$$

We rewrite Eq. (1) more compactly as follows:

$$\boldsymbol{y}_t = \boldsymbol{A}\boldsymbol{z}_t + \boldsymbol{H}\boldsymbol{\eta}_t, \quad \boldsymbol{\eta}_t \sim \mathcal{N}(\boldsymbol{0}, \boldsymbol{\Sigma}),$$

with $\boldsymbol{\eta}_t$ denoting structural errors. Note that the relation between reduced-form errors $\boldsymbol{\epsilon}_t$ and structural errors $\boldsymbol{\eta}_t$ is given by $\boldsymbol{\epsilon}_t = \boldsymbol{H}\boldsymbol{\eta}_t$.

By exploiting the fact that $\boldsymbol{\eta}_t = \boldsymbol{H}^{-1}\boldsymbol{\epsilon}_t$, and the lower triangular structure of $\boldsymbol{H}^{-1}$, we estimate the system equation-by-equation as a set of unrelated regressions, see Carriero et al. (2019). The first equation in Eq. (1) is:

$$y_{1t} = \boldsymbol{A}_{1\bullet}\boldsymbol{z}_t + \eta_{1t}, \quad \eta_{1t} \sim \mathcal{N}(0, \sigma_1^2),$$

where $\boldsymbol{A}_{1\bullet}$ refers to the first row in $\boldsymbol{A}$. The mth (for $m = 2, \dots, M$) equation of Eq. (1) is:

$$y_{mt} = \boldsymbol{A}_{m\bullet}\boldsymbol{z}_t - \sum_{i=1}^{m-1} h_{mi}^{-1}\epsilon_{it} + \eta_{mt}, \quad \eta_{mt} \sim \mathcal{N}(0, \sigma_m^2),$$

where $\boldsymbol{A}_{m\bullet}$ refers to the mth row in $\boldsymbol{A}$ and h_{mi}^{-1} to the (m, i)th element in $\boldsymbol{H}^{-1}$. To simplify the mth equation, we define the $K_m \times 1$-vectors $\boldsymbol{\alpha}_m = (\boldsymbol{A}'_{m\bullet}, \{h_{mi}^{-1}\}_{i=1}^{m-1})'$ and $\tilde{\boldsymbol{z}}_{mt} = (\boldsymbol{z}'_t, \{\epsilon_{it}\}_{i=1}^{m-1})'$ and write

$$y_{mt} = \boldsymbol{\alpha}'_m\tilde{\boldsymbol{z}}_{mt} + \eta_{mt}, \quad \eta_{mt} \sim \mathcal{N}(0, \sigma_m^2). \tag{A.1}$$

Note that, if $m = 1$, $\boldsymbol{\alpha}_1 = A_{1\bullet}$ and $\tilde{\boldsymbol{z}}_{1t} = \boldsymbol{z}_t$. To define the Eq. (A.1) in terms of full data matrices, let $\boldsymbol{y}_m$ be a $T \times 1$-vector, $\tilde{\boldsymbol{Z}}_m$ a $T \times K_m$ matrix and $\boldsymbol{\eta}_m$ a $T \times 1$-vector, collecting y_{mt}, $\tilde{\boldsymbol{z}}'_{mt}$ and η_{mt} on the tth position, respectively. The following equation, conditional on $S_t(u_{t-1})$, denotes a standard linear regression model:

$$\boldsymbol{y}_m = \tilde{\boldsymbol{Z}}_m\boldsymbol{\alpha}_m + \boldsymbol{\eta}_m, \quad \boldsymbol{\eta}_m \sim \mathcal{N}(\boldsymbol{0}, \sigma_m^2\boldsymbol{I}_T).$$

Appendix B. Posterior distributions and sampling algorithm

In this Appendix we briefly summarize the main steps involved for posterior inference. Given the model likelihood and prior assumptions we can derive a standard Markov Chain Monte Carlo (MCMC) algorithm, which iterates through conditional posterior distributions. The symbol $\star$ indicates that we condition on all other parameters of the model (including the state indicator $S_t(u_{t-1})$).

1. We draw $\boldsymbol{\alpha}_m$, for $m = 1, \dots, M$, from a multivariate Normal distribution:

   $$\boldsymbol{\alpha}_m|\star = \mathcal{N}(\bar{\boldsymbol{\alpha}}_m, \bar{\boldsymbol{\Omega}}_m),$$

   with $\bar{\boldsymbol{\alpha}}_m$ denoting the posterior mean and $\bar{\boldsymbol{\Omega}}_m$ refering to the posterior variance-covariance matrix. Both quantities are of well-known form an given by:

   $$\begin{aligned} \bar{\boldsymbol{\alpha}}_m &= \bar{\boldsymbol{\Omega}}_m\big(\tilde{\boldsymbol{Z}}'_m\boldsymbol{y}_m/\sigma_m^2 + \underline{\boldsymbol{\Omega}}_m^{-1}\underline{\boldsymbol{\alpha}}_m\big), \\ \bar{\boldsymbol{\Omega}}_m &= \big(\tilde{\boldsymbol{Z}}'_m\tilde{\boldsymbol{Z}}_m/\sigma_m^2 + \underline{\boldsymbol{\Omega}}_m^{-1}\big)^{-1}, \end{aligned}$$

   with the $K_m \times 1$-vector $\underline{\boldsymbol{\alpha}}_m$ being a prior mean and the $K_m \times K_m$-matrix $\underline{\boldsymbol{\Omega}}_m$ a diagonal prior variance covariance matrix. In the following, the prior quantities collect the equation-specific elements defined by the hierarchical prior. That is, $\underline{\boldsymbol{\alpha}}_m$ collects the respective elements of $\tilde{\boldsymbol{a}}$, defined in Eq. (3), elements of the lower Cholesky factor are centered on zero from Eq. (4), $\underline{\boldsymbol{\Omega}}_m$ collects the respective elements of $\{\tilde{v}_{1j}\}_{j=1}^{J}$, $\{\tilde{v}_{0j}\}_{j=1}^{J}$ and $\{\hat{v}_{0j}\}_{j=1}^{J}$.[18]
2. We sample the structural error variances $\{\sigma_m^2\}_{m=1}^{M}$ from an inverse Gamma distribution:

   $$\sigma_m|\star \sim \mathcal{G}^{-1}(d_m, D_m),$$

   with $d_m = (T/2 + 3)$ denoting the posterior degrees of freedom and $D_m = (\boldsymbol{\eta}'_m\boldsymbol{\eta}_m/2 + 0.3)$ refering to the posterior scaling parameter.

[18] In particular, for the mth equation, $\underline{\boldsymbol{\alpha}}_m = (\{\tilde{a}_j\}_{j\in S_m}, \{\tilde{a}_j\}_{j\in S_m}, \boldsymbol{0}'_{m-1})'$, where $\tilde{a}_j$ denotes the jth element in $\tilde{\boldsymbol{a}}$ and $\boldsymbol{0}_{m-1}$ refers to $(m-1) \times 1$-vector of zeros, while $\underline{\boldsymbol{\Omega}}_m = \text{diag}(\{\tilde{v}_{1s}\}_{s\in\tilde{S}_m}, \{\tilde{v}_{0s}\}_{s\in\tilde{S}_m}, \{\hat{v}_q\}_{q\in Q_m})$. Here, $\tilde{S}_m = \{k(m-1)+1, \dots, km\}$ is a set of indicators of cardinality $k = (MP + 2)$ that serves to select the equation-specific coefficients and the set Q_m of cardinality $(m-1)$ selects the prior indicators corresponding to equation-specific elements of the lower Cholesky factor.

3. To update the hierarchical priors we rely on steps outlined next. First, note that that Eqs. (2) and (3) can be written as a random coefficient specification for each parameter. That is,

$$a_{ij} = \tilde{a}_j + \tilde{v}_{ij}, \quad \tilde{v}_{ij} \sim \mathcal{N}(0, \tilde{v}_{ij})$$
$$\tilde{a}_j = a_j + v_j, \quad v_j \sim \mathcal{N}(0, v_j).$$

with $i \in \{0, 1\}$ and $j = 1, \dots, J$.
The (hyper)parameters of the hierarchical shrinkage prior are sampled from the following conditional posterior distributions:

- The HS scaling parameters of the lowest hierarchy (i.e., $\tilde{v}_j = \tilde{\lambda}_i^2 \tilde{\psi}_{ij}^2$) are obtained by using the methods outlined in Makalic and Schmidt (2015). That is, for $i \in \{0, 1\}$ and $j = 1, \dots, J$, sampling the local $\tilde{\psi}_{ij}^2$ and the global shrinkage parameter $\tilde{\lambda}_i^2$ involves producing draws from four independent inverse Gamma distributions. For the $\tilde{\psi}_{ij}^2$ the distribution is given by:

$$\tilde{\psi}_{ij}^2 | \star \sim \mathcal{G}^{-1}\left(1, \frac{1}{\tilde{\zeta}_{ij}} + \frac{(a_{ij} - \tilde{a}_j)^2}{2\tilde{\lambda}_i^2}\right),$$

  the global shrinkage parameter is sample from:

$$\tilde{\lambda}_i^2 | \star \sim \mathcal{G}^{-1}\left(\frac{J+1}{2}, \frac{1}{\tilde{\xi}_i} + \sum_{j=1}^{J} \frac{(a_{ij} - \tilde{a}_j)^2}{2\tilde{\psi}_{ij}^2}\right),$$

  while the two auxiliary variables $\tilde{\zeta}_{ij}$ and $\tilde{\xi}_i$ are drawn from:

$$\tilde{\zeta}_{ij} | \star \sim \mathcal{G}^{-1}(1, 1 + 1/\tilde{\psi}_{ij}^2),$$
$$\tilde{\xi}_i | \star \sim \mathcal{G}^{-1}(1, 1 + 1/\tilde{\lambda}_i^2).$$

- Similar to the lowest hierarchy we also defined a HS prior on the top one. To sample the scaling parameters ψ_j^2 (local scaling) and λ^2 (global scaling), we therefore rely on exactly the same steps outlined in the four equations above. This can be done by replacing $(a_{ij} - \tilde{a}_j)^2$ with $(\tilde{a}_j - a_j)^2$, $\tilde{\lambda}_i$ with λ and $\tilde{\zeta}_{ij}$ with ζ_j in the respective equations.
- In a next step, we update the hierarchical (common) prior mean $\tilde{\boldsymbol{a}}$ element-wise from a Gaussian distribution:

$$\tilde{a}_j | \star \sim \mathcal{N}(\bar{a}_j, \bar{v}_j),$$

  for $j = 1, \dots, J$. The posterior mean $\bar{a}_j$ and variance $\bar{v}_j$ are given by:

$$\bar{v}_j = \left(\left(\frac{1}{\tilde{v}_{1j}} + \frac{1}{\tilde{v}_{0j}}\right) + \frac{1}{v_j}\right)^{-1},$$
$$\bar{a}_j = \bar{v}_j\left(\left(\frac{a_{1j}}{\tilde{v}_{1j}} + \frac{a_{0j}}{\tilde{v}_{0j}}\right) + \frac{a_j}{v_j}\right).$$

4. The HS hyperparameters of elements associated with the covariances are sampled from:

$$\hat{\psi}_r^2 | \star \sim \mathcal{G}^{-1}\left(1, \frac{1}{\hat{\zeta}_r} + \frac{h_r^2}{2\hat{\lambda}^2}\right),$$

  the global shrinkage parameter is sampled from:

$$\hat{\lambda}^2 | \star \sim \mathcal{G}^{-1}\left(\frac{R+1}{2}, \frac{1}{\hat{\xi}} + \sum_{r=1}^{R} \frac{h_r^2}{2\hat{\psi}_r^2}\right),$$

  while the two auxiliary variables are drawn from:

$$\hat{\zeta}_r | \star \sim \mathcal{G}^{-1}(1, 1 + 1/\hat{\psi}_r^2),$$
$$\hat{\xi} | \star \sim \mathcal{G}^{-1}(1, 1 + 1/\hat{\lambda}^2).$$

5. Finally, following Alessandri and Mumtaz (2019) (see their Appendix for the ST-VAR), we sample the threshold parameters in one block using a random walk Metropolis Hastings step. We therefore use two independent Gaussian proposal densities to sample candidate values for γ and ϕ:

$$\gamma^{(*)} \sim \mathcal{N}(\gamma^{(s)}, c_\gamma), \quad \phi^{(*)} \sim \mathcal{N}(\phi^{(s)}, c_\phi).$$

Here, $\gamma^{(*)}$ refers to the candidate value and $\gamma^{(s)}$ to the last accepted draw of γ, while $\phi^{(*)}$ denotes the proposed value and $\phi^{(s)}$ the last accepted draw of ϕ. In the following, the acceptance probability ω is given by the ratio of the posterior

likelihood of the proposed values $(\gamma^{(*)}, \phi^{(*)})$ and the posterior likelihood of the last accepted values $(\gamma^{(s)}, \phi^{(s)})$, since both proposal are symmetric. That is,

$$\omega = \min\left(1, \frac{\mathcal{L}(\gamma^{(*)}, \phi^{(*)}|\star)p(\gamma^{(*)})p(\phi^{(*)})}{\mathcal{L}(\gamma^{(s)}, \phi^{(s)}|\star)p(\gamma^{(s)})p(\phi^{(s)})}\right),$$

with $\mathcal{L}$ denoting the conditional data likelihood. Note that the prior of γ is defined as a truncated Gaussian distribution implying that the acceptance probability of the hyperparameter pair $(\gamma^{(*)}, \phi^{(*)})$ is zero, if $\gamma^{(*)} < \min(z_t)$ or $\gamma^{(*)} > \max(z_t)$ as these values obtain zero support per construction. In the empirical application, we choose c_γ and c_ϕ in such a way to obtain an acceptance rate between 25 to 40%.

We repeat these steps 32,000 times and discard the initial 2,000 draws as a burn-in. We consider each 10th of the retained draws, resulting in a set of 3,000 independent draws from the posterior for inference.

Appendix C. Data sources and transformations

Table C1
Dataset.

Variable	Description	Source	Trans.
	Financial variables		
E3M	Euribor 3-month rate, monthly percentage	SDW	
GBY2	EA 2-year government bond yield, monthly percentage	SDW	
GBY10	EA 10-year government bond yield, monthly percentage	SDW	
ES50	Euro Stoxx 50, price index, monthly	SDW	$100\cdot\log(x)$
OAS	ICE BofA Euro high yield index option-adjusted spread (OAS), monthly percentage	FRED	
	Macroeconomic variables		
HICP	Harmonised index of consumer prices monthly index, w.d.a, s.a.	SDW	$100\cdot\log(x)$, yoy
UNEMP	Harmonized Unemployment Rate monthly, s.a.	FRED	
IP	Industrial production, excl. construction monthly, w.d.a, s.a.	SDW	$100\cdot\log(x)$, yoy
EPU	Economic policy uncertainty, monthly	BBD	$100\cdot\log(x)$
	Expectations/survey-based variables		
ISICI	Industrial confidence indicator, monthly percentage	SDW	
CSCCI	Consumer confidence indicator, monthly percentage	SDW	
CSU12	Consumer unemployment expectations over next 12 months, monthly, percentage	SDW	
CIE	Consumer opinion future tendency of inflation monthly, s.a.	FRED	$x/10^{\dagger}$

Notes: Column *Trans.* indicates the transformation applied to the respective series x. †Transformed to correspond to the scale of HICP inflation. FRED indicates the database maintained by the Federal Reserve Bank of St. Louis (fred.stlouisfed.org), SDW is the statistical data warehouse by the European Central Bank (ECB, sdw.ecb.europa.eu). The abbreviation *s.a.* is short for seasonally adjusted, *w.d.a.* means working-day adjusted (both only stated if applicable), *yoy* refers to year-on-year differenced data. *BBD* is short for Baker et al. (2016), who provide the economic policy uncertainty index on their webpage: policyuncertainty.com.

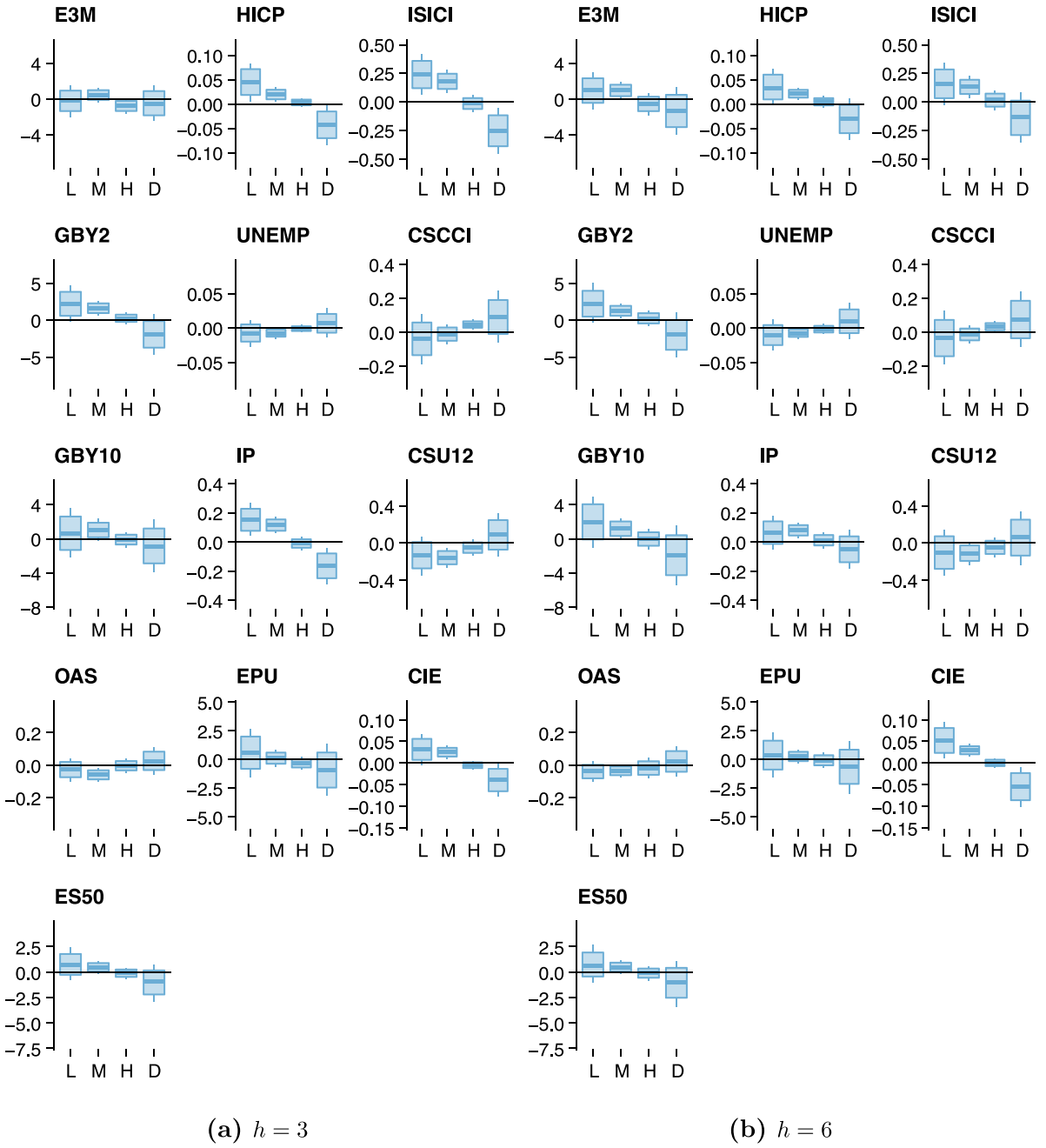

Fig. D.1. Boxplots of the impulse response functions to the target/policy rate shock for different levels of uncertainty at one-quarter and six-months ahead. Impulse response functions are summarized in form of a boxplot. The rectangle marks the 25th and 75th percentile of the posterior distribution (interquartile range), the posterior median is indicated as solid line; the whiskers of the plot refer to the 68% posterior credible set. Panel (a) shows responses on impact, panel (b) at the 12 month horizon. We display responses in the low (L), medium (M) or high (H) uncertainty state, as well as the difference (D) in responses between L and H. The L, M, H scenarios are based on the $\{0.05, 0.5, 0.95\}$ unconditional quantile of the uncertainty indicator over time. A description of the variables and transformations is provided in Appendix C.

Appendix D. Additional empirical results

Table D.1
Summary of the impulse response functions for low and high level of uncertainty on impact and one-year ahead.

Variable	h = 0						h = 12					
	TG		FG		QE		TG		FG		QE	
	L	H	L	H	L	H	L	H	L	H	L	H
Financial												
E3M	−1.437	−0.769	−0.321	−0.459	−0.026	0.494	1.844	0.440	−0.597	−1.201	−0.048	−0.549
	(−2.323, −0.730)	(−1.135, −0.417)	(−0.655, −0.013)	(−0.914,0.010)	(−1.015,0.908)	(−1.157,2.104)	(−0.284,3.873)	(−1.062,1.832)	(−1.213,0.050)	(−2.849,0.558)	(−1.911,1.592)	(−6.307,5.230)
GBY2	1.715	1.250	−1.073	−1.585	−1.769	1.993	2.236	0.240	−0.589	−1.032	−0.049	−0.141
	(0.025,3.337)	(0.723,1.748)	(−1.527, −0.717)	(−2.189, −0.919)	(−3.063, −0.505)	(−0.195,4.202)	(−0.118,4.608)	(−0.885,1.372)	(−1.347,0.076)	(−2.411,0.286)	(−1.954,1.949)	(−5.083,4.229)
GBY10	2.061	0.173	−0.274	−1.635	−2.989	−0.045	1.025	0.061	−0.305	−1.008	−0.503	−0.454
(0.330,3.689)	(−0.326,0.686)	(−0.711,0.163)	(−2.287, −0.996)	(−4.225, −1.830)	(−2.133,2.090)		(−1.216,3.431)	(−1.210,1.335)	(−1.003,0.380)	(−2.354,0.293)	(−2.528,1.249)	(−5.897,3.994)
OAS	−0.223	−0.011	0.013	−0.001	0.024	0.019	−0.025	−0.041	0.006	−0.017	0.024	0.104
	(−0.282, −0.159)	(−0.029,0.007)	(−0.003,0.029)	(−0.025,0.023)	(−0.025,0.073)	(−0.062,0.103)	(−0.070,0.018)	(−0.106,0.015)	(−0.004,0.017)	(−0.092,0.054)	(−0.009,0.058)	(−0.143,0.367)
ES50	1.226	−0.220	0.320	−0.554	−0.050	0.177	0.796	−0.002	0.097	−0.222	−0.116	−0.198
	(0.558,1.975)	(−0.555,0.104)	(0.166,0.558)	(−0.972, −0.149)	(−0.910,0.870)	(−1.238,1.641)	(−0.570,2.449)	(−0.697,0.642)	(−0.270,0.535)	(−1.005,0.493)	(−1.380,1.055)	(−3.007,2.269)
Macroeconomic												
HICP	0.025	−0.002	−0.011	0.005	−0.006	0.016	0.014	0.006	0.001	−0.008	−0.004	0.013
	(0.004,0.045)	(−0.008,0.004)	(−0.016, −0.005)	(−0.003,0.012)	(−0.021,0.010)	(−0.011,0.043)	(−0.015,0.043)	(−0.005,0.018)	(−0.006,0.010)	(−0.021,0.006)	(−0.028,0.020)	(−0.033,0.062)
UNEMP	−0.008	0.000	0.000	−0.001	−0.001	−0.023	−0.014	−0.006	0.002	−0.001	0.003	−0.014
	(−0.020,0.003)	(−0.003,0.004)	(−0.003,0.003)	(−0.005,0.004)	(−0.010,0.009)	(−0.039, −0.006)	(−0.036,0.006)	(−0.016,0.003)	(−0.004,0.008)	(−0.011,0.010)	(−0.012,0.020)	(−0.054,0.027)
IP	0.152	−0.028	0.003	0.034	0.139	−0.171	−0.033	0.045	0.009	−0.011	−0.045	−0.107
	(0.048,0.259)	(−0.057,0.005)	(−0.027,0.030)	(−0.009,0.074)	(0.050,0.215)	(−0.307, −0.029)	(−0.125,0.056)	(−0.008,0.100)	(−0.012,0.035)	(−0.074,0.046)	(−0.123,0.022)	(−0.329,0.101)
EPU	0.558	0.003	−1.171	0.918	0.765	−0.775	0.325	−0.169	0.176	−0.212	−0.012	0.983
	(−1.589,2.628)	(−0.651,0.716)	(−1.747, −0.586)	(0.088,1.725)	(−0.956,2.440)	(−3.626,2.013)	(−1.076,1.711)	(−0.919,0.548)	(−0.178,0.543)	(−1.096,0.708)	(−1.065,1.085)	(−2.052,4.234)
Expectations												
ISICI	0.291	−0.008	−0.022	−0.016	−0.093	0.336	0.041	0.072	−0.003	−0.007	−0.060	−0.058
	(0.193,0.384)	(−0.039,0.022)	(−0.046,0.003)	(−0.053,0.021)	(−0.170, −0.005)	(0.209,0.464)	(−0.093,0.183)	(−0.009,0.155)	(−0.035,0.035)	(−0.102,0.083)	(−0.182,0.041)	(−0.379,0.263)
CSCCI	−0.154	0.058	0.020	−0.028	−0.005	0.026	−0.045	0.027	0.006	0.021	−0.018	−0.035
	(−0.223, −0.085)	(0.037,0.079)	(0.002,0.039)	(−0.055,0.000)	(−0.060,0.052)	(−0.072,0.120)	(−0.143,0.055)	(−0.006,0.060)	(−0.019,0.034)	(−0.015,0.058)	(−0.105,0.057)	(−0.173,0.104)
CSU12	−0.246	−0.084	0.007	0.000	−0.320	0.145	−0.113	−0.105	0.010	−0.024	0.040	0.032
	(−0.436, −0.059)	(−0.149, −0.023)	(−0.050,0.057)	(−0.080,0.081)	(−0.487, −0.158)	(−0.116,0.400)	(−0.341,0.092)	(−0.204, −0.018)	(−0.047,0.062)	(−0.134,0.085)	(−0.137,0.229)	(−0.377,0.440)
CIE	0.041	−0.006	−0.006	−0.007	−0.017	−0.033	0.032	0.002	−0.003	−0.004	−0.011	0.015
	(0.020,0.063)	(−0.013,0.000)	(−0.012,0.000)	(−0.015,0.002)	(−0.036, −0.001)	(−0.063, −0.003)	(0.005,0.062)	(−0.007,0.013)	(−0.011,0.004)	(−0.016,0.007)	(−0.035,0.011)	(−0.025,0.057)

Notes: The table shows median posterior responses at the given time horizons as well as the 75% posterior credible interval in parantheses. The low (L) and high (H) uncertainty scenarios are based on the {0.05, 0.95} unconditional quantile of the uncertainty indicator over time. A description of the variables and transformations is provided in Appendix C.

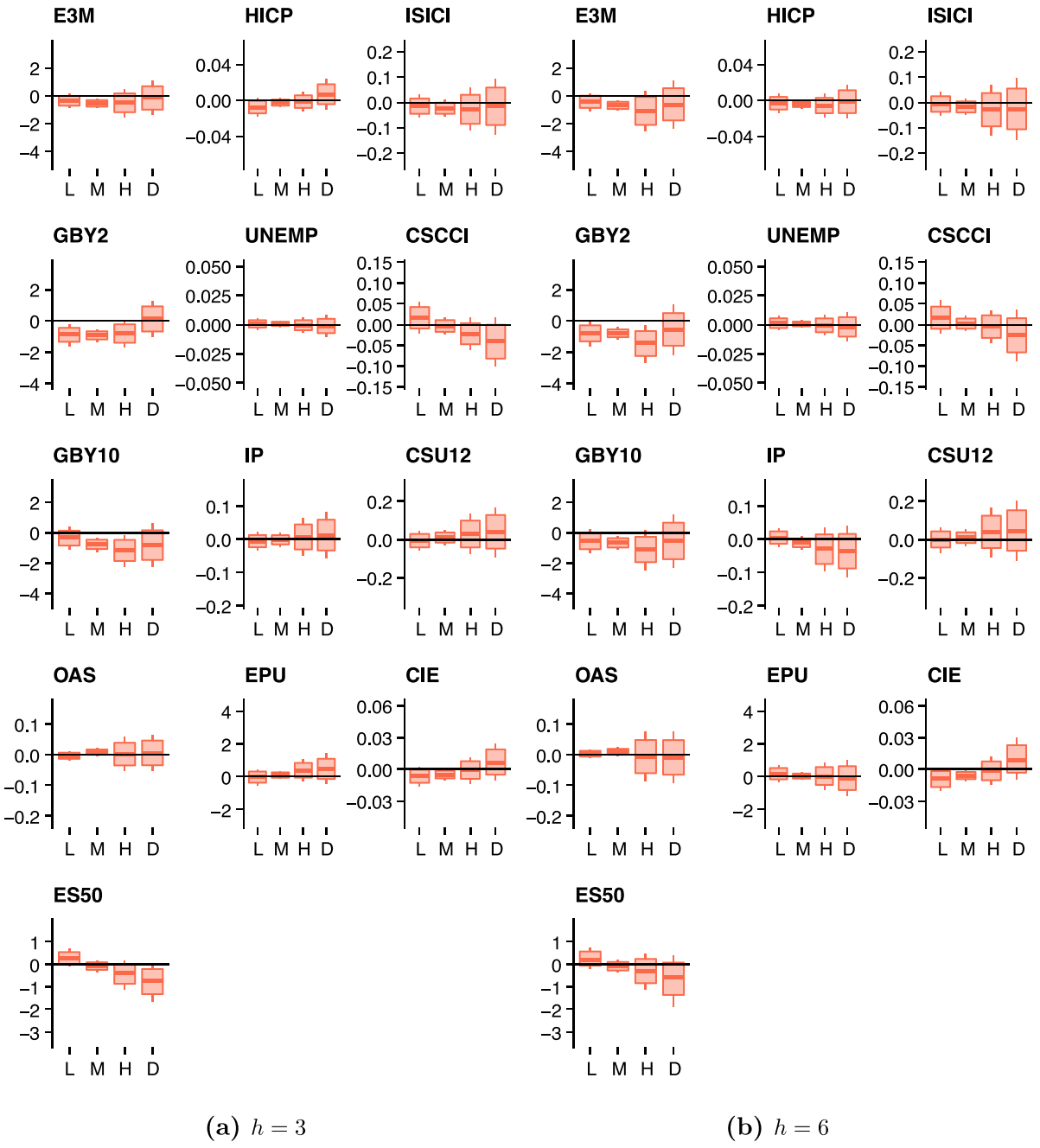

Fig. D.2. Boxplots of the impulse response functions to the forward guidance shock for different levels of uncertainty at one-quarter and six-months ahead. Impulse response functions are summarized in form of a boxplot. The rectangle marks the 25th and 75th percentile of the posterior distribution (interquartile range), the posterior median is indicated as solid line; the whiskers of the plot refer to the 68% posterior credible set. Panel (a) shows responses on impact, panel (b) at the 12 month horizon. We display responses in the low (L), medium (M) or high (H) uncertainty state, as well as the difference (D) in responses between L and H. The L, M, H scenarios are based on the $\{0.05, 0.5, 0.95\}$ unconditional quantile of the uncertainty indicator over time. A description of the variables and transformations is provided in Appendix C.

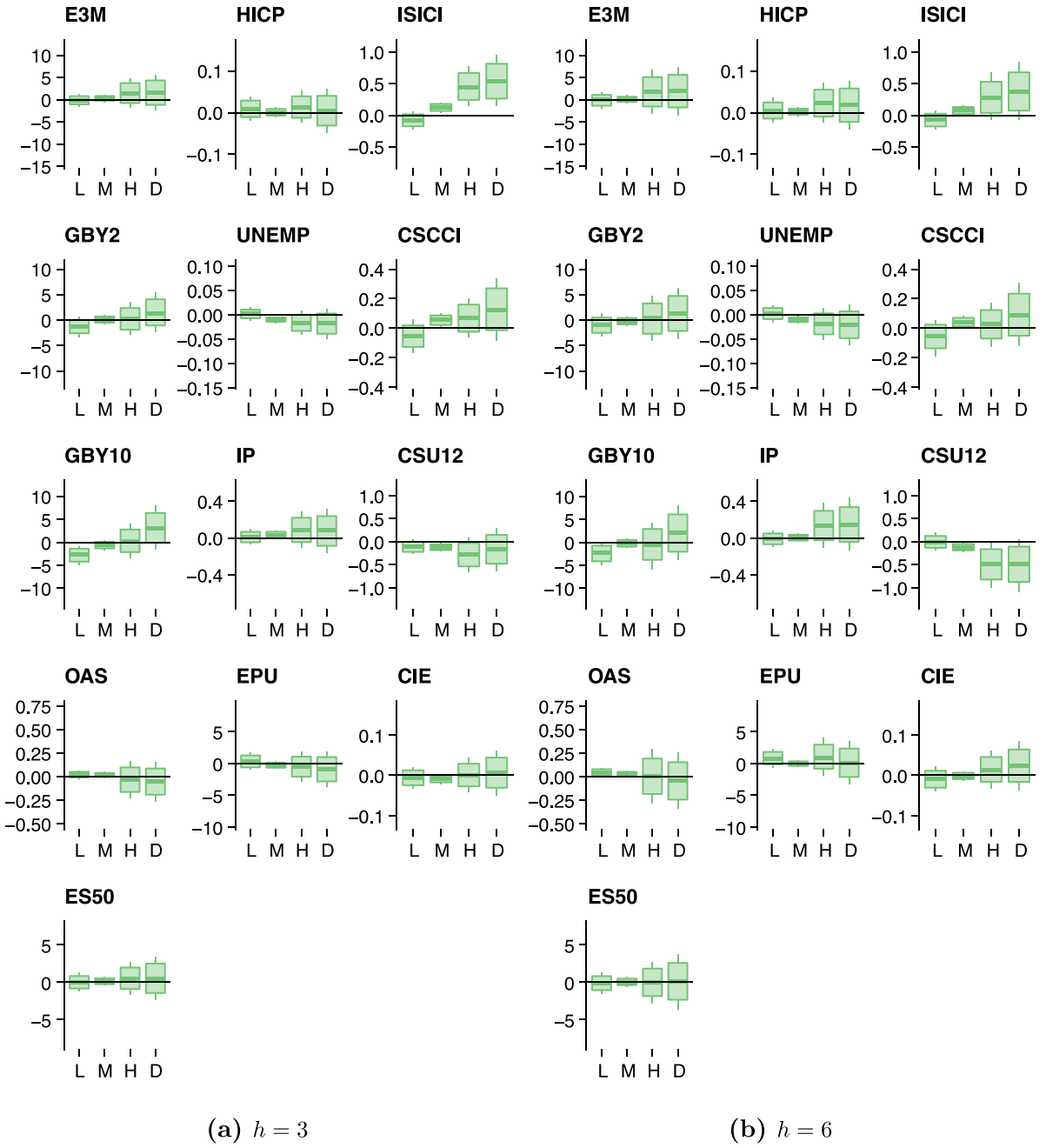

Fig. D.3. Boxplots of the impulse response functions to the quantitative easing shock for different levels of uncertainty at one-quarter and six-months ahead. Impulse response functions are summarized in form of a boxplot. The rectangle marks the 25th and 75th percentile of the posterior distribution (interquartile range), the posterior median is indicated as solid line; the whiskers of the plot refer to the 68% posterior credible set. Panel (a) shows responses on impact, panel (b) at the 12 month horizon. We display responses in the low (L), medium (M) or high (H) uncertainty state, as well as the difference (D) in responses between L and H. The L, M, H scenarios are based on the $\{0.05, 0.5, 0.95\}$ unconditional quantile of the uncertainty indicator over time. A description of the variables and transformations is provided in Appendix C.

Supplementary material

Supplementary material associated with this article can be found, in the online version, at 10.1016/j.jebo.2021.09.041.

References

Aastveit, K.A., Natvik, G.J., Sola, S., 2017. Economic uncertainty and the influence of monetary policy. J. Int. Money Finance 76, 50–67.
Alessandri, P., Mumtaz, H., 2019. Financial regimes and uncertainty shocks. J. Monet. Econ. 101, 31–46.
Altavilla, C., Brugnolini, L., Gürkaynak, R.S., Motto, R., Ragusa, G., 2019. Measuring euro area monetary policy. J. Monet. Econ. 108, 162–179.
Andrade, P., Ferroni, F., 2021. Delphic and odyssean monetary policy shocks: evidence from the euro area. J. Monet. Econ. 117, 816–832.
Angrist, J.D., Jordà, O., Kuersteiner, G.M., 2018. Semiparametric estimates of monetary policy effects: string theory revisited. J. Bus. Econ. Stat. 36 (3), 371–387.
Arellano, C., Bai, Y., Kehoe, P.J., 2019. Financial frictions and fluctuations in volatility. J. Polit. Economy 127 (5), 2049–2103.
Auerbach, A.J., Gorodnichenko, Y., 2012. Measuring the output responses to fiscal policy. Am. Econ. J. 4 (2), 1–27.
Azqueta-Gavaldón, A., Hirschbühl, D., Onorante, L., Saiz, L., 2020. Economic policy uncertainty in the euro area: an unsupervised machine learning approach. ECB Working Paper 2359.
Baker, S.R., Bloom, N., Davis, S.J., 2016. Measuring economic policy uncertainty. Q. J. Econ. 131 (4), 1593–1636.
Bauer, M.D., Swanson, E.T., 2020. The Fed's response to economic news explains the "Fed Information Effect". National Bureau of Economic Research (NBER) Working Paper 27013.
Bech, M.L., Gambacorta, L., Kharroubi, E., 2014. Monetary policy in a downturn: are financial crises special? International Finance 17 (1), 99–119.
Bekaert, G., Hoerova, M., Lo Duca, M., 2013. Risk, uncertainty and monetary policy. J. Monet. Econ. 60 (7), 771–788. https://EconPapers.repec.org/RePEc:eee:moneco:v:60:y:2013:i:7:p:771-788
Berger, D., Dew-Becker, I., Giglio, S., 2020. Uncertainty shocks as second-moment news shocks. Rev. Econ. Stud. 87 (1), 40–76.
Bernanke, B.S., Boivin, J., Eliasz, P., 2005. Measuring the effects of monetary policy: a factor-augmented vector autoregressive (FAVAR) approach. Q. J. Econ. 120 (1), 387–422.
Bernanke, B.S., Kuttner, K.N., 2005. What explains the stock market's reaction to federal reserve policy? J. Finance 60 (3), 1221–1257.
Bloom, N., 2009. The impact of uncertainty shocks. Econometrica 77 (3), 623–685.
Boivin, J., Kiley, M.T., Mishkin, F.S., 2010. Chapter 8 – how has the monetary transmission mechanism evolved over time? In: Friedman, B.M., Woodford, M. (Eds.) Handbook of Monetary Economics, vol. 3. Elsevier, pp. 369–422.
Borio, C.E.V., Hofmann, B., 2017. Is monetary policy less effective when interest rates are persistently low? BIS Working Paper 628.
Brand, C., Buncic, D., Turunen, J., 2010. The impact of ECB monetary policy decisions and communication on the yield curve. J. Eur. Econ. Assoc. 8 (6), 1266–1298.
Burriel, P., Galesi, A., 2018. Uncovering the heterogeneous effects of ECB unconventional monetary policies across euro area countries. Eur. Econ. Rev. 101, 210–229.
Cadonna, A., Frühwirth-Schnatter, S., Knaus, P., 2020. Triple the gamma–a unifying shrinkage prior for variance and variable selection in sparse state space and TVP models. Econometrics 8 (2), 20.
Caggiano, G., Castelnuovo, E., Groshenny, N., 2014. Uncertainty shocks and unemployment dynamics in US recessions. J. Monet. Econ. 67, 78–92.
Caggiano, G., Castelnuovo, E., Nodari, G., 2017. Uncertainty and monetary policy in good and bad times. Bank of Finland Research Discussion Paper 2017-06.
Caldara, D., Fuentes-Albero, C., Gilchrist, S., Zakrajšek, E., 2016. The macroeconomic impact of financial and uncertainty shocks. Eur. Econ. Rev. 88, 185–207.
Campbell, J.R., Evans, C.L., Fisher, J.D.M., Justiniano, A., 2012. Macroeconomic effects of federal reserve forward guidance. Brookings Pap. Econ. Act. 2012, 1–80.
Carriero, A., Clark, T.E., Marcellino, M., 2019. Large Bayesian vector autoregressions with stochastic volatility and non-conjugate priors. J. Econom. 212 (1), 137–154.
Carriero, A., Clark, T.E., Marcellino, M.G., 2018. Endogenous Uncertainty. Federal reserve bank of cleveland working paper 18-05.
Carvalho, C.M., Polson, N.G., Scott, J.G., 2010. The horseshoe estimator for sparse signals. Biometrika 97 (2), 465–480.
Chan, J.C.C., Eisenstat, E., Strachan, R.W., 2020. Reducing the state space dimension in a large TVP-VAR. J. Econom. 218 (1), 105–118.
Clark, T.E., 2011. Real-time density forecasts from Bayesian vector autoregressions with stochastic volatility. J. Bus. Econ. Stat. 29 (3), 327–341.
Cogley, T., Sargent, T.J., 2005. Drifts and volatilities: monetary policies and outcomes in the post WWII US. Rev. Econ. Dyn. 8 (2), 262–302.
Coibion, O., Gorodnichenko, Y., Kumar, S., 2018. How do firms form their expectations? new survey evidence. Am. Econ. Rev. 108 (9), 2671–2713.
Coibion, O., Gorodnichenko, Y., Weber, M., 2019. Monetary policy communications and their effects on household inflation expectations. National Bureau of Economic Research (NBER) Working Paper 25482.
Cui, W., Sterk, V., 2019. Quantitative easing. HKIMR Working Paper 08/2019.
Dahlhaus, T., 2017. Conventional monetary policy transmission during financial crises: an empirical analysis. J. Appl. Econom. 32 (2), 401–421.
Davidson, S. N., Koop, G., Beckmann, J., & Schüssler, R. (2020). Measuring international spillovers in uncertainty and their impact on the economy. Manuscript,.
Doan, T., Litterman, R., Sims, C., 1984. Forecasting and conditional projection using realistic prior distributions. Econom. Rev. 3 (1), 1–100.
Fischer, M. M., Hauzenberger, N., Huber, F., & Pfarrhofer, M. (2021). General Bayesian time-varying parameter VARs for predicting government bond yields. arXiv preprint arXiv:2102.13393.
Gefang, D., Strachan, R., 2009. Nonlinear impacts of international business cycles on the UK–a Bayesian smooth transition VAR approach. Stud. Nonlinear Dyn. Econom. 14 (1).
Gertler, M., Karadi, P., 2015. Monetary policy surprises, credit costs, and economic activity. Am. Econ. J. 7 (1), 44–76.
Granger, C.W.J., Terasvirta, T., 1993. Modelling non-linear economic relationships. Oxford University Press, New York.
Gürkaynak, R.S., Sack, B.P., Swanson, E.T., 2005. Do actions speak louder than words? The response of asset prices to monetary policy actions and statements. Int. J. Cent. Bank. 1 (1).
Hauzenberger, N., Huber, F., Pfarrhofer, M., Zörner, T.O., 2021. Stochastic model specification in Markov switching vector error correction models. Stud. Nonlinear Dyn. Econom. 25 (2).
Hauzenberger, N., Pfarrhofer, M., 2021. Bayesian state-space modeling for analyzing heterogeneous network effects of US monetary policy. Scandinavian Journal of Economics. in-press
Huber, F., Zörner, T.O., 2019. Threshold cointegration in international exchange rates: a Bayesian approach. Int. J. Forecast. 35 (2), 458–473.
Hutchinson, J., Smets, F., 2017. Monetary policy in uncertain times: ECB monetary policy since june 2014. Manchester Sch. 85, e1–e15.
Jannsen, N., Potjagailo, G., Wolters, M.H., 2019. Monetary policy during financial crises: is the transmission mechanism impaired? Int. J. Cent. Bank. 15 (4), 81–126.
Jarociński, M., Karadi, P., 2020. Deconstructing monetary policy surprises–the role of information shocks. Am. Econ. J. 12 (2), 1–43.
Jarociński, M., Lenza, M., 2018. An inflation-predicting measure of the output gap in the euro area. J. Money Credit Bank. 50 (6), 1189–1224.
Jordà, O., 2005. Estimation and inference of impulse responses by local projections. Am. Econ. Rev. 95 (1), 161–182.
Kashyap, A.K., Stein, J.C., 2000. What do a million observations on banks say about the transmission of monetary policy? Am. Econ. Rev. 90 (3), 407–428.
Kuttner, K.N., 2001. Monetary policy surprises and interest rates: evidence from the fed funds futures market. J. Monet. Econ. 47 (3), 523–544.
Kuttner, K.N., 2018. Outside the box: unconventional monetary policy in the great recession and beyond. J. Econ. Perspect. 32 (4), 121–146.

Leduc, S., Liu, Z., 2016. Uncertainty shocks are aggregate demand shocks. J. Monet. Econ. 82, 20–35.
Litterman, R.B., 1986. Forecasting with Bayesian vector autoregressions – five years of experience. J. Bus. Econ. Stat. 4 (1), 25–38.
Ludvigson, S., Ma, S., Ng, S., 2020. Uncertainty and business cycles: exogenous impulse or endogenous response? Am. Econ. J.. in-press
Makalic, E., Schmidt, D.F., 2015. A simple sampler for the horseshoe estimator. IEEE Signal Process. Lett. 23 (1), 179–182.
Miranda-Agrippino, S., Ricco, G., 2021. The transmission of monetary policy shocks. Am. Econ. J. 13 (3), 74–107.
Mishkin, F.S., 1996. The channels of monetary transmission: lessons for monetary policy. Technical Report. National Bureau of Economic Research.
Nakamura, E., Steinsson, J., 2018. High-frequency identification of monetary non-neutrality: the information effect. Q. J. Econ. 133 (3), 1283–1330.
Paul, P., 2020. The time-varying effect of monetary policy on asset prices. Rev. Econ. Stat. 102 (4), 690–704.
Plagborg-Møller, M., Wolf, C.K., 2021. Local projections and VARs estimate the same impulse responses. Econometrica 89 (2), 955–980.
Primiceri, G.E., 2005. Time varying structural vector autoregressions and monetary policy. Rev. Econ. Stud. 72 (3), 821–852.
Ramey, V.A., Zubairy, S., 2018. Government spending multipliers in good times and in bad: evidence from US historical data. J. Polit. Economy 126 (2), 850–901.
Rossi, B., Sekhposyan, T., 2017. Macroeconomic uncertainty indices for the euro area and its individual member countries. Empir. Econ. 53 (1), 41–62.
Sims, C.A., Zha, T., 2006. Were there regime switches in US monetary policy? Am. Econ. Rev. 96 (1), 54–81.
Swanson, E.T., 2021. Measuring the effects of federal reserve forward guidance and asset purchases on financial markets. J. Monet. Econ. 118, 32–53.
Tenreyro, S., Thwaites, G., 2016. Pushing on a string: US monetary policy is less powerful in recessions. Am. Econ. J. 8 (4), 43–74.
Woodford, M., 2005. Central bank communication and policy effectiveness. National Bureau of Economic Research (NBER) Working Paper 11898.